axioms

MDPI

Article

Closed-Form Orbits for a Six-Parameter 3D Dynamical System Using the Multistage Optimal Homotopy Perturbation Method

Remus-Daniel Ene [1], Romeo Negrea [1], Rodica Badarau [2] and Nicolina Pop [3,*]

[1] Department of Mathematics, Politehnica University of Timisoara, 300006 Timisoara, Romania; remus.ene@upt.ro (R.-D.E.); romeo.negrea@upt.ro (R.N.)
[2] Department of Mechanical Machines, Equipment and Transportation, Politehnica University of Timisoara, 300222 Timisoara, Romania; rodica.badarau@upt.ro
[3] Department of Physical Foundations of Engineering, Politehnica University of Timisoara, 300223 Timisoara, Romania
* Correspondence: nicolina.pop@upt.ro

Abstract

Numerous systems in electrical engineering, biology, and mechanical structures can be modeled using dynamical systems theory. This paper examines the behavior of a 3D dynamical system with six parameters, specifically its damped or periodic oscillations and asymptotic properties as functions of six physical parameters. The system is integrated explicitly through a smooth solution of a third order nonlinear differential equation, yielding exact parametric expressions that describe a heteroclinic orbit. To analyze parameter influence, we apply the Multistage Optimal Homotopy Perturbation Method (MOHPM). Its main advantage is the small number of iterations required, due to the effective choice of auxiliary convergence control functions. The MOHPM solutions agree closely with numerical results, demonstrated qualitatively through figures and quantitatively through tables. Accuracy is further assessed by comparison with the Optimal Homotopy Perturbation Method (OHPM). A qualitative analysis of errors is also provided.

Keywords: multistage optimal homotopy perturbation method; dynamical system; damped oscillations; asymptotic behaviors; heteroclinic orbits

MSC: 37B65; 37C79; 65H20; 37J06; 37J35; 65L99

1. Introduction

In the study of natural phenomena for various fields such as physics, chemistry, biology, engineering, etc., an important role is played by nonlinear problems modeled by nonlinear differential equations. The effort of researchers is oriented towards finding efficient numerical methods to solve various types of nonlinear differential equations with a large number of unknowns and which have a strong nonlinearity. Chaos is a complex and widely studied nonlinear phenomenon, being identified by some of its fundamental characteristics [1], such as dense periodic orbits, topological mixing, etc. Nonlinear dynamical systems that exhibit chaotic behavior are sensitive to the initial conditions. Chaotic behavior is found in a variety of systems, used in electrical circuits, fluid dynamics, mechanical devices, lasers, the time evolution of the magnetic field of celestial bodies, the dynamics of molecular vibrations, population growth in ecology, weather forecasting [2]. Since the first chaotic attractor was reported by Lorenz [3], researchers have focused their attention on generating chaotic behavior in simple autonomous systems for

Check for updates

Academic Editor: Pranali Roy Chowdhury

Received: 29 May 2026
Revised: 20 July 2026
Accepted: 27 July 2026
Published: 2 August 2026

Copyright: © 2026 by the authors. Licensee MDPI, Basel, Switzerland. This article is an open access article distributed under the terms and conditions of the Creative Commons Attribution (CC BY) license.

potential technological applications [4]. In this process, there are two stationary research directions. The first is the generation of a hyperchaotic system with at least two positive Lyapunov exponents [5,6]. Another important research direction is the construction of chaotic attractors with complicated topological structures, such as ring-scroll and multi-scroll chaotic attractors [4].

The chaotic properties were a priority for many researchers, without taking into account their other particularities, as: the existence of periodical/almost periodical orbits, for example.

In theory, the dynamics of some 3D systems are characterized by periodical or almost periodical behaviors or by asymptotic behaviors or damped oscillations, against the existence of stable equilibrium points. Lazureanu [7–9] studied only the geometrical properties: the Hamilton-Poisson structure, symmetries, equilibrium points. Other systems are examined by Biggs et al. [10], Gholamin et al. [11], Xu et al. [12], and so on. Such 3D systems can be explicitly integrate, via two well-known techniques. The first technique consists in existence of two first integrals (H- the Hamiltonian and C- the independently Casimir functional) and writing the exact solution as the intersection between surfaces $H(x,y,z) = cst_1$ and $C(x,y,z) = cst_2$, respectively. The second technique consists in reduction of the dynamic system to one nonlinear ordinary differential equation (ODE), just facilitating writing the solution of the dynamic system in the form of exact parametric solutions, via an unknown smooth function. In the second situation both first integrals are unknown or only one first integral is known. Generally, the dynamical systems of dimension greater than 4 cannot be explicitly integrated, via an unknown smooth function.

Analytical methods to find homoclinic and heteroclinic orbits were proposed by Bao et al. [13] and Dessoky et al. [14] using the series expansion method directly on initial system or for one differential equation corresponding to the reduction of the dynamic system. Recently, Li et al. [15] developed a new technique to study homoclinic orbits with multiple pulses. They analytically investigated a 3D piecewise linear forced oscillation systems taking into consideration the Shil'nikov hypotheses and non-Shil'nikov hypotheses.

In literature, the concept "exact parametric solutions" can also be found to other researchers such as Harko et al. [16]. The initial system was reduced to a nonlinear ODE depending on one unknown function. A similar approach can be found in the work [17] using an unknown function, namely the Weierstrass function.

Iterative techniques are generally used to solve dynamic systems of nonlinear equations. When the nonlinearity of the problems considered is strong, the convergence of iterations is cumbersome. With recent advances in the research of nonlinear problems, analytical techniques for solving nonlinear equations have been developed. However, most current methods base their solution methodology on the assumption of small nonlinearities, which limits their use in solving physical and engineering applications [18]. Among the asymptotic methods used to find approximate solutions to highly nonlinear problems are [18]: variational iteration method (VIM), homotopic perturbation method (HPM), energy balance, parameter expansion, Hamiltonian approach and homotopic analysis method, Adomian decomposition (ADM), improved amplitude-frequency formulation, max-min approach, The HPM method developed by the Chinese mathematician He in 1998 [19–21] is not limited by the assumption of small nonlinearities and has been used with very good results in many applications in science and engineering to find approximate solutions to nonlinear differential equations. Thus HPM combines the traditional perturbation method with the homotopy theory used in topology and uses a simple initial analytical solution that gradually approximates the solution of the differential equation by a parameter that converges to unity and thus a complex problem is decomposed into a series of simple problems that simplify the derivation of approximate solutions. The main goal is to improve the convergence, accuracy, and stability of nonlinear

and fractional differential equations, especially on long time intervals. HPM is an asymptotic method with bounded convergence outside the initial conditions of the equation [2,18,22–24]. Finding accurate and efficient techniques to overcome the limitations of HPM has long been an active research activity. To overcome this weakness, HPM must be applied on intervals. For example, Abbasbandy used this approach to solve the Riccati equation [25]. Hashim and Chowdhury developed another method for solving a system of nonlinear differential equations over multiple intervals, a method called the multistage homotopic perturbation method (MHPM) [23–25]. MHPM treats standard HPM as an algorithm on successive time subintervals, transmitting the final value of one interval as the initial condition of the next. This considerably improves the long-term accuracy for chaotic systems such as Lorenz, Chen, Lü and hyperchaotic Lü–Chen systems. Based on the MHPM, Gökdogan and Merdan derived an approximate solution for the nonlinear Coullet differential equation [26]. Wang and Yu extended the use of MHPM to obtain approximate numerical-analytic solutions of the chaotic fractional-order Chen system, as well as the hyperchaotic fractional-order Lorenz system with numerical simulations showing good accuracy at long time scales [27]. An efficient MHPM for fractional Lotka-Volterra derivatives extends this idea to fractional Caputo derivatives and shows that the fractional order significantly affects the trajectory velocity [27].

The multistage optimal homotopy perturbation method (MOHPM) introduces an auxiliary linear operator into the homotopy asymptotic method (HAM) and optimizes it by minimizing the residual error, providing faster and more reliable convergence than the standard HPM and optimal HAM for strongly nonlinear ODEs in fluid dynamics [28]. In this paper, we consider a three-dimensional chaotic system with cubic nonlinearity. Three-dimensional nonlinear dynamical systems with six parameters represent a class of compact generators capable of producing complex chaotic dynamics. They are frequently used in applications such as multistable secure communications, generating robust chaos over extended parameter ranges, and implementing electronic circuits [1]. The study of these systems is usually carried out by methods specific to nonlinear dynamics, and they are often proposed as fundamental components in the development of circuits for communications and secure encryption [1,5]. In these dynamical systems, some fundamental dynamical properties are studied, such as the equilibrium point, the phase portrait, the Lyapunov exponent, the Kaplan-Yorke dimension, the stability and bifurcation of equilibria using the central manifold theorem, the Routh-Hurwitz criterion, the fork bifurcation theory, the Hopf bifurcation and the Lyapunov function, the Poincare application [4–6].

The engineering utility of the proposed chaotic system could be identified in [29], while [30] presented a system identification study of a servo-valve-controlled hydraulic cylinder. This setup operates under variable loads, typical of hydraulic actuators used in wind turbine blade pitch systems.

This paper contains 5 sections. Section 1 Introduction highlighted the motivation to investigate the dynamical system according to state-of-art. The study of dynamical systems with cubic nonlinearities, taking into account of the Routh-Hurwitz criterion, is presented in Section 2. Section 3 is dedicated details of the Multistage Optimal Homotopy Perturbation Method (MOHPM). Results and comparison with corresponding numerical ones and OHPM results, respectively, are provided in Section 4. Conclusions are summarized in the last Section 5.

2. Closed-Form Solutions for 3D Dynamical System with Cubic Nonlinearity

By considering the six-parameters dynamical system shown in [4]:

$$\begin{cases} \dot{x} = -a\,x + b\,yz \\ \dot{y} = -c\,y^3 + d\,xz \\ \dot{z} = e\,z - f\,xy \end{cases}, \tag{1}$$

with the initial conditions

$$x(0) = x_{i0} \quad , \quad y(0) = y_{i0} \quad , \quad z(0) = z_{i0} \, , \tag{2}$$

where a, b, c, d, e, $f > 0$ are dimensionless physical parameters, we propose to explicitly integrate it.

The equilibrium points of the System (1) are: $P_0(0,0,0)$, $P_1(\frac{e}{f}\sqrt{\frac{ac}{bd}}, \sqrt{\frac{ae}{bf}}, \frac{a}{b}\sqrt{\frac{ce}{fd}})$, $P_2(-\frac{e}{f}\sqrt{\frac{ac}{bd}}, \sqrt{\frac{ae}{bf}}, -\frac{a}{b}\sqrt{\frac{ce}{fd}})$, $P_3(-\frac{e}{f}\sqrt{\frac{ac}{bd}}, -\sqrt{\frac{ae}{bf}}, \frac{a}{b}\sqrt{\frac{ce}{fd}})$ and $P_4(\frac{e}{f}\sqrt{\frac{ac}{bd}}, -\sqrt{\frac{ae}{bf}}, -\frac{a}{b}\sqrt{\frac{ce}{fd}})$.

The matrix of linear part of System (1) around the equilibrium point $P^*(x^*, y^*, z^*)$ is:

$$J(x^*, y^*, z^*) = \begin{pmatrix} -a & bz^* & by^* \\ dz^* & -3c(y^*)^2 & dx^* \\ -fy^* & -fx^* & e \end{pmatrix} . \tag{3}$$

The Jacobian matrix $J(P^*)$ defined by Equation (3) has the characteristic polynomial:

$$p_{J(P^*)}(\lambda) = \lambda^3 + \widetilde{\alpha}_2\lambda^2 + \widetilde{\alpha}_1\lambda + \widetilde{\alpha}_0 \, , \tag{4}$$

where $\widetilde{\alpha}_0 = -3ace(y^*)^2 + adf(x^*)^2 + bde(z^*)^2 + 2bdfx^*y^*z^* + 3bcf(y^*)^4$, $\widetilde{\alpha}_1 = 3c(a-e)(y^*)^2 - ae + bf(y^*)^2 + df(x^*)^2 - bd(z^*)^2$, $\widetilde{\alpha}_2 = 3c(y^*)^2 + a - e$.

For each point $P^*(x^*, y^*, z^*) \neq P_0(0,0,0)$ these coefficients become $\widetilde{\alpha}_0 = \frac{4a^2ce^2}{bf} > 0$, $\widetilde{\alpha}_1 = \frac{2ace}{bf}(a-e) > 0$ iff $a > e$, $\widetilde{\alpha}_2 = 3c\frac{ae}{bf} + a - e > 0$.

Taking into consideration the Routh–Hurwitz criterion, only for

$$(\mathrm{H}) \quad \widetilde{\alpha}_2 > 0, \, \widetilde{\alpha}_1 > 0, \, \widetilde{\alpha}_0 > 0 \text{ and } \widetilde{\alpha}_2\widetilde{\alpha}_1 - \widetilde{\alpha}_0 > 0 \, , \tag{5}$$

all the roots have negative real parts, so the equilibrium points $P^*(x^*, y^*, z^*) \neq P_0(0,0,0)$ are asymptotically stable.

Remark 1. *If the characteristic polynomial $p_{J(P^*)}(\lambda)$ admits the roots $\lambda_1 = \theta_1 < 0$ and $\lambda_{2,3} = \pm i\theta$ (the real part is zero), then the characteristic polynomial becomes*

$$p_{J(P^*)}(\lambda) = (\lambda - \lambda_1)(\lambda^2 + \theta^2) \, ,$$

whence $\widetilde{\alpha}_0 = -\lambda_1\theta^2 > 0$, $\widetilde{\alpha}_1 = \theta^2 > 0$, $\widetilde{\alpha}_2 = -\lambda_1 > 0$, but $\widetilde{\alpha}_2\widetilde{\alpha}_1 - \widetilde{\alpha}_0 = 0$. Related to each point $P^*(x^*, y^*, z^*) \neq P_0(0,0,0)$ this condition involves a relation between physical constants, namely $c = \frac{bf}{3ae}\frac{-a^2+4ae-e^2}{a-e} > 0$. In this situation the equilibrium point $P^*(x^*, y^*, z^*) \neq P_0(0,0,0)$ becomes spectral stable.

The next proposition assures that the System (1) with initial data (2) can be explicitly integrate.

Proposition 1. *System (1) is explicitly solved via a smooth function $v : [0, \infty) \to \mathbb{R}^*$ using assumption (H) introduced by Equation (5):*

$$\begin{cases} x = \pm\frac{1}{\sqrt{2f(a+e)}}\sqrt{2ev - v'} \\ y = \pm\frac{1}{\sqrt{4bf}}\frac{-v'' + 2(-a+e)v' + 4aev}{\sqrt{(2ev - v')(2av + v')}} \\ z = \pm\frac{1}{\sqrt{2b(a+e)}}\sqrt{2av + v'} \end{cases} , \tag{6}$$

(the minus sign is chosen if the initial condition has the negative value) with v unknown smooth function, solution of the following problem:

$$\begin{cases} \frac{1}{2}[-v''' + 2(-a+e)v'' + 4aev'](2ev - v')(2av + v') - \\ \frac{1}{4}[-v'' + 2(-a+e)v' + 4aev][(2ev' - v'')(2av + v') + (2ev - v')(2av' + v'')] = \\ -\frac{c}{8bf}[-v'' + 2(-a+e)v' + 4aev]^3 + \frac{d}{2(a+e)}(2ev - v')^2(2av + v')^2 \,, \\ v(0) = fx_{i0}^2 + bz_{i0}^2 \,, \;\; v'(0) = 2b(a+e)z_{i0}^2 - 2av(0) \,, \\ v''(0) = 2b(a+e)[2(a+e)z_{i0}^2 - 2fx_{i0}y_{i0}z_{i0}] - 4av'(0) - 4a^2v(0) \,. \end{cases} \tag{7}$$

Proof. A simple combination between the first two equations from System (1) yields to

$$\frac{d}{dt}(fx^2 + bz^2) = -2a(fx^2 + bz^2) + 2b(a+e)z^2 \,,$$

whereas

$$fx^2 + bz^2 = e^{-2at}\left(\mathcal{C}_1 + \int_0^t 2b(a+e)z^2e^{2as}\,ds\right) \,,$$

with $\mathcal{C}_1 = fx_{i0}^2 + bz_{i0}^2 > 0$.

Hence, there is an unknown smooth function $w(t)$ such that:

$$\begin{aligned} fx^2(t) &= \tfrac{1}{2}e^{-2at}\varphi(t) + w(t) \,, \\ bz^2(t) &= \tfrac{1}{2}e^{-2at}\varphi(t) - w(t) \,, \end{aligned} \tag{8}$$

with $\varphi(t) = \mathcal{C}_1 + \int_0^t 2b(a+e)z^2e^{2as}\,ds$.

Now, the first equation from System (1) becomes

$$fx\dot{x} = -afx^2 + bfxyz \,,$$

and using fx^2 from Equation (8) we get

$$xyz = \tfrac{1}{bf}\left(aw + \tfrac{1}{2}w' + \tfrac{1}{4}e^{-2at}\varphi'\right) . \tag{9}$$

The third equation from System (1) can be rewritten as

$$\frac{1}{2}\frac{d}{dt}(bz^2) = bez^2 - bfxyz \,,$$

and substituting xyz given by Equation (9) we obtain

$$-\frac{a}{2}e^{-2at}\varphi + \frac{1}{4}e^{-2at}\varphi' = \frac{e}{2}e^{-2at}\varphi - ew - aw - \frac{1}{4}e^{-2at}\varphi' \,,$$

whence

$$w = \tfrac{1}{2}e^{-2at}\left(\varphi - \tfrac{1}{a+e}\varphi'\right) . \tag{10}$$

The first derivative of the smooth function w is

$$w' = \left(-a\varphi + \tfrac{3a+e}{2(a+e)}\varphi' - \tfrac{1}{2(a+e)}\varphi''\right)e^{-2at} \,. \tag{11}$$

By replacing $w(t)$ and $w'(t)$ from Equations (10) and (11) into the Equations (8) and (9) we obtain

$$\begin{aligned} fx^2(t) &= e^{-2at}\varphi(t) - \tfrac{1}{2(a+e)}\varphi'(t)e^{-2at}\,, \\ bz^2(t) &= \tfrac{1}{2(a+e)}\varphi'(t)\,, \\ xyz &= \tfrac{1}{bf}\left[\tfrac{1}{2}\varphi'(t) - \tfrac{1}{4(a+e)}\varphi''(t)\right]e^{-2at}\,. \end{aligned} \tag{12}$$

From expression xyz from Equation (12) we derived

$$y^2 = \frac{1}{bf}\frac{\left[\frac{1}{2}\varphi'(t)e^{-2at} - \frac{1}{4(a+e)}\varphi''(t)e^{-2at}\right]^2}{\frac{1}{2(a+e)}\varphi'(t)e^{-2at}\left(e^{-2at}\varphi(t) - \frac{1}{2(a+e)}\varphi'(t)e^{-2at}\right)}\,. \tag{13}$$

At this moment the unknown smooth function $v(t)$ is introduced by $v(t) = e^{-2at}\varphi(t)$, whereas the following relations hold:

$$\begin{aligned} e^{-2at}\varphi'(t) &= v'(t) + 2av(t)\,, \\ e^{-2at}\varphi''(t) &= v''(t) + 4av'(t) + 4a^2v(t)\,, \end{aligned} \tag{14}$$

and $v(0) = \varphi(0)$.

Substituting Equation (14) into Equations (12) and (13) we get

$$\begin{aligned} fx^2(t) &= \tfrac{1}{2(a+e)}(2ev - v')\,, \\ bz^2(t) &= \tfrac{1}{2(a+e)}(2av + v')\,, \\ y^2 &= \frac{1}{4bf}\frac{[-v'' + 2(-a+e)v' + 4aev]^2}{(2ev - v')(2av + v')} \end{aligned} \tag{15}$$

and, from here the desired results described in Equation (6) are deduces.

The second equation from System (1) becomes

$$\frac{1}{2}\frac{d}{dt}(y^2) = -cy^4 + d\,xyz\,,$$

and using Equations (12) and (15) it obtain

$$\begin{aligned} &\frac{d}{dt}\left\{\frac{1}{4bf}\frac{[-v'' + 2(-a+e)v' + 4aev]^2}{(2ev - v')(2av + v')}\right\} = \\ &-2c\left\{\frac{1}{4bf}\frac{[-v'' + 2(-a+e)v' + 4aev]^2}{(2ev - v')(2av + v')}\right\}^2 + \frac{2d}{bf}\left[\frac{1}{2}(v' + 2av) - \frac{1}{4}(v'' + 4av' + 4a^2v)\right]\,, \end{aligned}$$

whence the desired results given by Equation (7) are deduced.

The initial conditions $v(0)$, $v'(0)$ and $v''(0)$ can be obtained from the Equations (12)–(14) as:

$$\begin{aligned} &\varphi'(0) = 2b(a+e)z_{i0}^2\ ,\ \ v'(0) = \varphi'(0) - 2av(0)\,, \\ &\varphi''(0) = 2b(a+e)[2(a+e)z_{i0}^2 - 2fx_{i0}y_{i0}z_{i0}]\ ,\ \ v''(0) = \varphi''(0) - 4av'(0) - 4a^2v(0)\,, \end{aligned}$$

and hence, the initial conditions form Equation (8) hold. □

If $\overline{v}_{MOHPM}$ is a MOHPM solution (i.e., a semi-analytical solution builded using MOHPM method) of the Equation (7) then the functions set $(\overline{x}_{MOHPM}, \overline{y}_{MOHPM}, \overline{z}_{MOHPM})$ obtained from Equation (6) is called the MOHPM solution of the System (1) describing a 3D curve (unnecessary closed), called closed-form orbit of the System (1).

3. Theoretical Approach of the Multistage Optimal Homotopy Perturbation Method (MOHPM)

This section describes the ideas of the OHPM as given in [31–33].

Assume the initial-value problem (IVP) in the form:

$$\mathcal{L}_j\left[V_j(t)\right] + g_j(t) + \mathcal{N}_j\left[V_j(t)\right] = 0, \qquad t \in I_j, \qquad j = 1, 2, \ldots N\,, \tag{16}$$

with the initial condition

$$V_j(\alpha_0) = \alpha_j^{(0)}, \ \ldots\ , \ \frac{d^{m-1}\,V_j}{d\,t^{m-1}}(\alpha_0) = \alpha_j^{(m-1)}\,, \tag{17}$$

where $\mathcal{L}_j$ and $\mathcal{N}_j$ are the linear and nonlinear operators, respectively, and I_j is domain of interest, $g_j(t)$ is an arbitrary known continuous function, $\alpha_0 \in I_j$ and $\alpha_j^{(m)}$ are given real numbers, $m \geq 1$ being the order of nonlinear differential equation.

For nonlinear Equation (16), it was built a family of equations:

$$\mathcal{H}_j\big(v_j(t,p)\big)\big) \equiv \mathcal{L}_j\big(v_j(t,p)\big) + g_j(t) + p\mathcal{N}_j\big(v_j(t,p)\big) = 0\,, \tag{18}$$

with $p \in [0,\ 1]$.

In the following, we propose the unknown function $v_j(t,p)$ in the particular form

$$v_j(t,p) = V_{j,0}(t) + pV_{j,1}(t)\,. \tag{19}$$

The homotopy map introduced by Equation (18) has the following properties:

$$\mathcal{H}_j\big(v_j(t,0)\big)\big) \equiv \mathcal{L}_j\left[V_{j,0}(t)\right] + g_j(t) = 0, \tag{20}$$

$$\mathcal{H}_j\big(v_j(t,1)\big)\big) \equiv \mathcal{L}_j\big(V_{j,0}(t) + V_{j,1}(t)\big)\big) + g_j(t) + \mathcal{N}_j\big(V_{j,0}(t) + V_{j,1}(t)\big)\big) = 0. \tag{21}$$

It is understood that $v_j(t,0) = V_{j,0}(t)$ holds for $p = 0$ and $v_j(t,1) = V_j(t)$ holds for $p = 1$. Thus, as p increases from 0 to 1, the solution $v_j(t,p)$ varies from $V_{j,0}(t)$ to the solution $V_j(t)$, where $V_{j,0}(t)$ is the initial guess which is known and computed from Equation (17) for $p = 0$:

$$\mathcal{L}_j\left[V_{j,0}(t)\right] + g_j(t) = 0, \quad V_{j,0}(\alpha_0) = \alpha_j^{(0)}, \ \ldots\ , \ \frac{d^{m-1}\,V_{j,0}}{d\,t^{m-1}}(\alpha_0) = \alpha_j^{(m-1)}\,. \tag{22}$$

Consequently, the first-order approximate solution can be written as

$$\overline{V}_j(t) = V_{j,0}(t) + V_{j,1}(t)\,. \tag{23}$$

The initial/boundary conditions become

$$\overline{V}_j(\alpha_0)) = \alpha_j^{(0)}, \ \ldots\ , \ \frac{d^{m-1}\,\overline{V}_j}{d\,t^{m-1}}(\alpha_0) = \alpha_j^{(m-1)}\,. \tag{24}$$

The nonlinear operator $\mathcal{N}_j$ has the following series expansion with respect to the parameter p:

$$\mathcal{N}_j\big(\overline{V}_j(t)\big) = \mathcal{N}_j\big(V_{j,0}(t)\big) + p\left[V_{j,1}\frac{\partial \mathcal{N}_j}{\partial \overline{V}_j}\big(V_{j,0}(t)\big) + V'_{j,1}\frac{\partial \mathcal{N}_j}{\partial \overline{V}_j'}\big(V_{j,0}(t)\big) + V''_{j,1}\frac{\partial \mathcal{N}_j}{\partial \overline{V}_j''}\big(V_{j,0}(t)\big) + \ldots\right] + \ldots\,. \tag{25}$$

The homotopy relation given by Equation (18) becomes

$$\mathcal{H}_j(v_j(t,p)) \equiv \mathcal{L}_j(V_j(t)) + g_j(t) + p \cdot \Big\{ \mathcal{N}_j(V_{j,0}(t)) + p\Big[V_{j,1} \frac{\partial \mathcal{N}_j}{\partial \overline{V}_j}(V_{j,0}(t)) + V'_{j,1} \frac{\partial \mathcal{N}_j}{\partial \overline{V}_j{}'}(V_{j,0}(t)) + V''_{j,1} \frac{\partial \mathcal{N}_j}{\partial \overline{V}_j{}''}(V_{j,0}(t)) + \ldots \Big] + \ldots \Big\} = 0\,. \tag{26}$$

Let $H^{(j)}_{i,k}(t,p)$ be an auxiliary functions. The following new homotopy relation is proposed:

$$\mathcal{H}_j(v_j(t,p)) = \mathcal{L}_j\big[V_{j,0}(t)\big] + g_j(t) + p \cdot \Big\{ \mathcal{L}_j\big[V_{j,1}(t)\big] + H^{(j)}_{1,0}(t, C_{j,k_1}) \cdot \mathcal{N}_j\big[V_{j,0}(t)\big] \Big\} + p^2 \cdot \Big[H^{(j)}_{2,0}(t, C_{j,k_1}) \times V_{j,1} \cdot \frac{\partial \mathcal{N}_j}{\partial \overline{V}_j}\big[V_{j,0}(t)\big] + H^{(j)}_{2,1}(t, C_{j,k_1}) \cdot V'_{j,1} \cdot \frac{\partial \mathcal{N}_j}{\partial \overline{V}_j{}'}\big[V_{j,0}(t)\big] + H^{(j)}_{2,2}(t, C_{j,k_1}) \cdot V''_{j,1} \cdot \frac{\partial \mathcal{N}_j}{\partial \overline{V}_j{}''}\big[V_{j,0}(t)\big] + \ldots \Big] + \ldots\,. \tag{27}$$

By using just one iteration of the OHPM method (see Equation (19)), terms in p^2 are neglected, to achieve accurate solutions.

From Equations (19) and (23), we obtain

$$v_j(t,0) = V_{j,0}(t), \qquad v_j(t,1) = \overline{V}(t). \tag{28}$$

Now, equating the coefficients of p^0 and p^1 into Equation (27), it holds that $V_{j,0}$ is given by Equation (22), and the first approximation $V_{j,1}(t)$ is obtained from the following equation:

$$\mathcal{L}_j\big[V_{j,1}(t)\big] + H^{(j)}_{1,0}(t, C_{j,k_1}) \cdot \mathcal{N}_j\big[V_{j,0}(t)\big] = 0,\ V_{j,1}(\alpha_0) = 0\,. \tag{29}$$

In the next, the nonlinear operator $\mathcal{N}_j\big[V_{j,0}(t)\big]$ that appear in Equation (29) has the general form

$$\sum_{i=1}^{m} h_{j,i}(t) g_{j,i}(t) K_{j,i}(t), \tag{30}$$

with the known functions $h_{j,i}(t)$, $g_{j,i}(t)$ and $K_{j,i}(t)$ depending on the initial guess $V_{j,0}(t)$ and nonlinear operator $\mathcal{N}_j$, m being a known integer.

For convenience the unknown function $V_{j,1}(t, C_{j,k_1})$ is chosen in the following forms:

$$V_{j,1}(t, C_{j,k_1}) = \sum_{k=1}^{n} \tilde{H}_{j,k}\Big(t, h_{j,i}(t), C_{j,k_1}\Big) g_{j,k}(t) K_{j,k}(t), \qquad k_1 = 1,\ 2,\ \ldots,\ s_1,\ \ j = 1,\ 2,\ \ldots,\ N\,, \tag{31}$$

or

$$V_{j,1}(t, C_{j,k_1}) = \sum_{k=1}^{n} \tilde{H}_{j,k}\Big(t, g_{j,i}(t), C_{j,k_1}\Big) h_{j,k}(t) K_{j,k}(t), \qquad k_1 = 1,\ 2,\ \ldots,\ s_1,\ \ j = 1,\ 2,\ \ldots,\ N\,, \tag{32}$$

$$V_{j,1}(\alpha_0) = 0,\ \ldots\,,\ \frac{d^{m-1}\, V_{j,1}}{d\, t^{m-1}}(\alpha_0) = 0\,. \tag{33}$$

The expression of the optimal auxiliary functions $\tilde{H}_{j,k}(t, h_{j,i}, C_{j,k_1})$ contains combinations of functions h_j and several unknown parameters C_{j,k_1}, $k_1 = 1,\ 2,\ \ldots,\ s_1$, and n is an arbitrary integer number. There are a lot a possibility to choose the value of the integer positive n and the optimal auxiliary functions $\tilde{H}_{j,k}$. The values of the parameters C_{j,k_1} can be optimally computed via the least-square method, namely by minimize the sum of squares:

$$\mathcal{E}_j = \sum_{i=1}^{N_{max}} \big[V_j(t_i) - V_{numerical}(t_i)\big]^2\,,\ j = 1, \ldots N\,, \tag{34}$$

where $\{t_i\,,\ i = \overline{1,\ N_{max}}\}$ is an arbitrary set of sampling points from I_j, N_{max} is an arbitrary integer greater than maximum of optimally parameters, $V_{numerical}$ denotes the numerical solution (assumed known) and computed via the fourth-order Runge-Kutta method using the Wolfram Mathematica software or MATLAB code.

Remark 2. *By integration of Equation (29) could be found several secular terms in the form* $t\cos(\omega_0 t)e^{-Kt}$, $t\sin(\omega_0 t)e^{-Kt}$ *or* te^{-Kt}, *and so on. Other secular terms as* $t\cos(\omega_0 t)$, $t\sin(\omega_0 t)$, $C_0 t$ *must be zero for avoid the resonance effect.*

Therefore, a first-order OHPM solution given by Equation (23) is well-defined for each interval I_j.

Next, changing the initial approximation $V_{j,0}$ in each subinterval $I_j = [t_{j-1},\ t_j)$ from the previous one, we can optimally compute the parameters C_{j,k_1} at $j = 1,\ 2,\ \ldots\ N$, $k_1 = 1,\ 2,\ \ldots,\ s_1$. For instant, we define $\alpha_j = V(t_j)$ in the subinterval $[t_{j-1},\ t_j)$.

Hence, the first-order approximate solution will be:

$$\overline{V}(t) = \begin{cases} V_1(t) = V_{1,0}(t) + V_{1,1}(t)\ , & t_0 \le t < t_1 \\ V_2(t) = V_{2,0}(t) + V_{2,1}(t)\ , & t_1 \le t < t_2 \\ \qquad\qquad \vdots & \\ V_N(t) = V_{N,0}(t) + V_{N,1}(t)\ , & t_{N-1} \le t < T\ . \end{cases} \tag{35}$$

For the points t_j, $j \ge 1$ the smoothing conditions are added:

$$V_j(t_j - 0) = V_{j+1}(t_j)\ ,\ \ldots\ ,\ \frac{d^{(m-1)}\ V_j}{d\ t^{(m-1)}}(t_j - 0) = \frac{d^{(m-1)}\ V_{j+1}}{d\ t^{(m-1)}}(t_j)\ ,\ m \ge 1\ . \tag{36}$$

The initial value problem' solution is semi-analytically calculated for extended value of T. For $j = 0$ the MOHPM convert to the standard OHPM. It is also important to highlight that MOHPM gives an easy way to adjust and control the convergence region by means of the auxiliary function $\tilde{H}_{j,k}$ involving many convergence-control parameters C_{j,k_1}. Then again, the proposed scheme overcomes the main difficulty, due to the extended computational domain, in calculating the solution of problem.

4. Results and Discussion

4.1. Semi-Analytical Solutions via MOHPM Technique

Based on the MOHPM procedure applied for obtaining semi-analytical solutions of the Equation (7), the damped oscillations are investigated according with Routh-Hurwitz's criterion for one set of physical parameters.

Firstly, it is defined the nonlinear operator $\mathcal{N}[v(t)]$ that appears in Equation (7) as:

$$\begin{array}{l} \mathcal{N}[v[t]] = \frac{1}{2}[-v''' + 2(-a+e)v'' + 4aev'](2ev - v')(2av + v') - \\ \frac{1}{4}[-v'' + 2(-a+e)v' + 4aev][(2ev' - v'')(2av + v') + (2ev - v')(2av' + v'')] - \\ \left\{ -\frac{c}{8bf}[-v'' + 2(-a+e)v' + 4aev]^3 + \frac{d}{2(a+e)}(2ev - v')^2(2av + v')^2 \right\}. \end{array} \tag{37}$$

Assumed that the physical parameters are $a = 2.096$, $b = 0.84$, $c = 0.275$, $d = 1.65$, $e = 0.23$, $f = 1.24$. The eigenvalues of the polynomial $p_{J(P^*)}(\lambda)$ defined by Equation (4) are $\lambda_1 = -2.07597308814$, $\lambda_{2,3} = -0.0859293545 \pm 0.3329276899\ i$.

The initial extended domain is proposed $I = [0,\ 80]$. We split this domain into three subintervals $I_1 = [0,\ 25]$, $I_2 = [25,\ 50]$, $I_3 = [50,\ 80]$. Using MOHPM procedure the first-order approximate solution $\overline{v}(t)$ is:

$$\overline{v}(t) = \begin{cases} v_1(t) = v_{1,0}(t) + v_{1,1}(t)\ , & t \in I_1 = [0,\ 25] \\ v_2(t) = v_{2,0}(t) + v_{2,1}(t)\ , & t \in I_2 = [25,\ 50] \\ v_3(t) = v_{3,0}(t) + v_{3,1}(t)\ , & t \in I_3 = [50,\ 80] \end{cases},$$

with $v_{1,0}(t)$, $v_{1,1}(t)$, $v_{2,0}(t)$, $v_{2,1}(t)$, $v_{3,0}(t)$, $v_{3,1}(t)$ are built below via OHPM method.

Related to the subinterval $I_1 = [0,\ 25]$ the System (1) has nonuniformly behavior.

For the first subinterval $I_1 = [t_0,\ t_1] = [0,\ 25]$, with $g_1 = 0$, we choose following operators that appear in Equation (16) as:

$$\mathcal{L}_1[v(t)] = v''' + (K^{(1)} + 2K_1^{(1)})v'' + [(K_1^{(1)})^2 + 2K^{(1)}K_1^{(1)} + (\omega_0^{(1)})^2]v' + [K^{(1)}(K_1^{(1)})^2 + K^{(1)}(\omega_0^{(1)})^2]v\,, \tag{38}$$

and

$$\mathcal{N}_1[v(t)] = \mathcal{N}[v(t)] - \left[v''' + (K^{(1)} + 2K_1^{(1)})v'' + [(K_1^{(1)})^2 + 2K^{(1)}K_1^{(1)} + (\omega_0^{(1)})^2]v' + [K^{(1)}(K_1^{(1)})^2 + K^{(1)}(\omega_0^{(1)})^2]v\right]. \tag{39}$$

The first-order OHPM solution $\overline{v}_1(t) = v_{1,0}(t) + v_{1,1}(t)$, is defined by Equation (23), with $v_{1,0}(t)$ solution of the Equation (22) taking into account the initial conditions from Equation (7):

$$v_{1,0}(t) = (M_1^{(1)}\cos(\omega_0^{(1)}t) + M_2^{(1)}\sin(\omega_0^{(1)}t))e^{-K_1^{(1)}t} + M_0^{(1)}e^{-K^{(1)}t}\,. \tag{40}$$

The expression of operator $\mathcal{N}_1[v_{1,0}(t)]$ from Equation (29) as in the Equation (30), where the product $g_{1,k}(t)h_{1,k}(t)$ is:

$$\begin{aligned} g_{1,k}(t)h_{1,k}(t) \in \Big\{ & 1\,,\ \cos(\omega_0^{(1)}t)e^{-K_1^{(1)}t}\,,\ \sin(\omega_0^{(1)}t)e^{-K_1^{(1)}t}\,,\ 1\cdot e^{-K^{(1)}t}\,,\ 1\cdot e^{-2K^{(1)}t}\,,\ 1\cdot e^{-2K_1^{(1)}t}\,, \\ & \cos(3\omega_0^{(1)}t)e^{-(K^{(1)}+K_1^{(1)})t}\,,\ \sin(3\omega_0^{(1)}t)e^{-(K^{(1)}+K_1^{(1)})t}\,,\ \cos(2\omega_0^{(1)}t)e^{-2K_1^{(1)}t}\,,\ \sin(2\omega_0^{(1)}t)e^{-2K_1^{(1)}t}\Big\}\,, \end{aligned} \tag{41}$$

and $K_{1,k}$ some real constants depending on $M_0^{(1)}$, $M_1^{(1)}$, $M_2^{(1)}$ and $\omega_0^{(1)}$. There are n = 10 elementary functions.

The first approximation $v_{1,1}(t)$ is defined in Equation (32), where the auxiliary functions $\tilde{H}_{1,k}\big(t, g_{1,i}(t), C_{1,k_1}\big)$, $k = 1,\ 2, \dots\ ,\ n = 10$, for $j = 1$, are chosen as:

$$\begin{aligned} &\tilde{H}_{1,1} = \tilde{C}_0\,, && \tilde{H}_{1,2} = (\tilde{S}_1 + \tilde{T}_1 t)\cos(\omega_0^{(1)}t)\,, && \tilde{H}_{1,3} = (\tilde{S}_2 + \tilde{T}_2 t)\sin(\omega_0^{(1)}t)\,, \\ &\tilde{H}_{1,4} = (\tilde{A}_0 + \tilde{T}_3 t)\,, && \tilde{H}_{1,5} = \tilde{A}_1\,, && \tilde{H}_{1,6} = \tilde{A}_2\,, \\ &\tilde{H}_{1,7} = \sum_{i=1}^{N_{max}} \tilde{D}_i\cos((2i-1)\omega_0^{(1)}t)\,, && \tilde{H}_{1,8} = \sum_{i=1}^{N_{max}} \tilde{E}_i\sin((2i-1)\omega_0^{(1)}t)\,, && \tilde{H}_{1,9} = \sum_{i=1}^{N_{max1}} \tilde{F}_i\cos((2i)\omega_0^{(1)}t)\,, \\ &\tilde{H}_{1,10} = \sum_{i=1}^{N_{max1}} \tilde{G}_i\sin((2i)\omega_0^{(1)}t)\,. \end{aligned}$$

Remark 3. *The above auxiliary functions will contribute to build the first approximation $v_{1,1}(t)$ such: by using the functions $g_{1,k}(t)h_{1,k}(t)$ into the Equations (29), (30), (38), and integrating them yields the first approximation $v_{1,1}(t)$ of the form given by Equation (32).*

The first-order approximate solution $\overline{v}_1(t)$, using OHPM method, is obtained by Equations (23), (32) and (47), for $j = 1$:

$$\begin{aligned} &\overline{v}_1(t) = v_{1,0}(t) + v_{1,1}(t) = C_0^{(1)} + (S_1^{(1)} + T_1^{(1)}t)\cos(\omega_0^{(1)}t)e^{-K_1^{(1)}t} + (S_2^{(1)} + T_2^{(1)}t)\sin(\omega_0^{(1)}t)e^{-K_1^{(1)}t} + \\ &A_1^{(1)}e^{-2K^{(1)}t} + A_2^{(1)}e^{-2K_1^{(1)}t} + \sum_{i=1}^{N_{max}}\Big(D_i^{(1)}\cos((2i-1)\omega_0^{(1)}t) + E_i^{(1)}\sin((2i-1)\omega_0^{(1)}t)\Big)e^{-(K^{(1)}+K_1^{(1)})t} + \\ &\sum_{i=1}^{N_{max1}}\Big(F_i^{(1)}\cos((2i)\omega_0^{(1)}t) + G_i^{(1)}\sin((2i)\omega_0^{(1)}t)\Big)e^{-2K_1^{(1)}t} + (A_0^{(1)} + T_3^{(1)}t)e^{-K^{(1)}t}\,, \end{aligned} \tag{42}$$

where all real parameters depending on $K_{1,k}$ will be optimally computed, via the least squares method (see Appendix A, Equation (A1)).

By integration of the Equation (29), the terms $\tilde{T}_1 t\cos(\omega_0^{(1)}t)$, $\tilde{T}_2 t\sin(\omega_0^{(1)}t)$, $\tilde{T}_3 te^{-K^{(1)}t}$ are obtained and they depend on linear operator $\mathcal{L}_1[v(t)]$.

Remark 4. *The above auxiliary functions $\tilde{H}_{1,k}\big(t, g_{1,i}(t), C_{1,k_1}\big)$ are not unique. For example,*

$$\tilde{H}_{1,1} = \tilde{C}_0\,, \quad \tilde{H}_{1,2} = (\tilde{S}_1 + \tilde{T}_1 t)\cos(\omega_0^{(1)} t)\,, \quad \tilde{H}_{1,3} = (\tilde{S}_2 + \tilde{T}_2 t)\sin(\omega_0^{(1)} t)\,,$$
$$\tilde{H}_{1,4} = (\tilde{A}_0 + \tilde{T}_3 t)\,, \quad \tilde{H}_{1,5} = \tilde{A}_1\,, \quad \tilde{H}_{1,6} = \tilde{A}_2\,,$$
$$\tilde{H}_{1,7} = \sum_{i=1}^{N_{max}} \tilde{D}_i \cos((2i-1)\omega_0^{(1)} t)\,, \quad \tilde{H}_{1,8} = \tilde{E}_1 \sin(3\omega_0^{(1)} t)\,, \quad \tilde{H}_{1,9} = \tilde{F}_1 \cos(2\omega_0^{(1)} t)\,,$$
$$\tilde{H}_{1,10} = \tilde{G}_1 \sin(2\omega_0^{(1)} t)\,,$$

and so on. They are chosen such as the products from Equations (30) and (32), namely $g_{1,k}(t)h_{1,k}(t)$ *and* $\tilde{H}_{1,k}(t, g_{1,i}(t), C_{1,k_1})h_{1,k}(t)$*, respectively, have same form.*

Related to the subinterval $I_2 = [t_1,\ t_2] = [25,\ 50]$ the behavior of the System (1) is uniformly.

For the subinterval $I_2 = [25,\ 50]$, with $g_2 = 0$, the operators $\mathcal{L}_2[v(t)]$ and $\mathcal{N}_2[v(t)]$ that appear in Equation (16) are choosing by:

$$\mathcal{L}_2[v(t)] = v''' + 2K_1^{(2)} v'' + ((K_1^{(2)})^2 + (\omega_0^{(2)})^2)v'\,,$$

and

$$\mathcal{N}_2[v(t)] = \mathcal{N}[v(t)] - \left[v''' + 2K_1^{(2)} v'' + ((K_1^{(2)})^2 + (\omega_0^{(2)})^2)v'\right]\,,$$

respectively.

The first-order approximate solution $\overline{v}_2(t)$ defined by Equation (23), for $j = 2$, is:

$$\overline{v}_2(t) = v_{2,0}(t) + v_{2,1}(t)\,.$$

The zero-th order approximate solution $v_{2,0}(t)$ is solution of the Equation (22), using the smoothing conditions given by Equation (36):

$$v_{2,0}(t) = (M_1^{(2)} \cos(\omega_0 t) + M_2^{(2)} \sin(\omega_0^{(2)} t))e^{-K_1^{(2)} t} + M_0^{(2)}\,. \tag{43}$$

The nonlinear operator $\mathcal{N}_2[v_{1,0}(t)]$ has an expression as in Equation (30), where the product $g_{2,k}(t)h_{2,k}(t)$ is:

$$g_{2,k}(t)h_{2,k}(t) \in \left\{1\,,\ \cos(\omega_0^{(2)} t)e^{-K_1^{(1)} t}\,,\ \sin(\omega_0^{(2)} t)e^{-K_1^{(1)} t}\,,\ 1 \cdot e^{-2K_1^{(1)} t}\,,\ \cos(3\omega_0^{(2)} t)e^{-K_1^{(1)} t}\,,\ \sin(3\omega_0^{(2)} t)e^{-K_1^{(1)} t}\,,\right.$$
$$\left.\cos(2\omega_0^{(2)} t)e^{-2K_1^{(1)} t}\,,\ \sin(2\omega_0^{(2)} t)e^{-2K_1^{(1)} t}\right\}\,,$$

and $K_{2,k}$ some real constants depending on $M_0^{(2)}$, $M_1^{(2)}$, $M_2^{(2)}$ and $\omega_0^{(2)}$.

There are $n = 8$ elementary functions.

Similarly as previous subinterval, the first approximation $v_{2,1}(t)$ is defined in Equation (32), where the auxiliary functions $\tilde{H}_{2,k}(t, g_{2,i}(t), C_{2,k_1})$, $k = 1,\ 2, \ldots,\ n = 8$, for $j = 2$, could be chosen as:

$$\tilde{H}_{1,1} = \tilde{C}_0\,, \quad \tilde{H}_{1,2} = (\tilde{S}_1 + \tilde{T}_1 t)\cos(\omega_0^{(2)} t)\,, \quad \tilde{H}_{1,3} = (\tilde{S}_2 + \tilde{T}_2 t)\sin(\omega_0^{(2)} t)\,,$$
$$\tilde{H}_{1,4} = \tilde{A}_2\,, \quad \tilde{H}_{1,5} = \sum_{i=1}^{N_{max}} \tilde{D}_i \cos((2i-1)\omega_0^{(2)} t)\,, \quad \tilde{H}_{1,6} = \sum_{i=1}^{N_{max}} \tilde{E}_i \sin((2i-1)\omega_0^{(2)} t)\,,$$
$$\tilde{H}_{1,7} = \sum_{i=1}^{N_{max1}} \tilde{F}_i \cos((2i)\omega_0^{(2)} t)\,, \quad \tilde{H}_{1,8} = \sum_{i=1}^{N_{max1}} \tilde{G}_i \sin((2i)\omega_0^{(2)} t)\,.$$

Therefore, the first-order approximate solution, using OHPM method, defined by Equation (23), becomes:

$$\overline{v}_2(t) = v_{2,0}(t) + v_{2,1}(t) = \tilde{C}_0 + (\tilde{S}_1 + \tilde{T}_1 t)\cos(\omega_0^{(2)} t)e^{-K_1^{(2)} t} + (\tilde{S}_2 + \tilde{T}_2 t)\sin(\omega_0^{(2)} t)e^{-K_1^{(2)} t} + \tilde{A}_2 e^{-2K_1^{(2)} t} + \sum_{i=1}^{N_{max}} \left(\tilde{D}_i \cos((2i-1)\omega_0^{(2)} t) + \tilde{E}_i \sin((2i-1)\omega_0^{(2)} t)\right) e^{-K_1^{(2)} t} + \sum_{i=1}^{N_{max1}} \left(\tilde{F}_i \cos((2i)\omega_0^{(2)} t) + \tilde{G}_i \sin((2i)\omega_0^{(2)} t)\right) e^{-2K_1^{(2)} t}, \quad (44)$$

where all real parameters depending on $K_{2,k}$ will be optimally computed, via the least squares method (see Appendix A, Equation (A2)).

The smoothing conditions are:

$$\overline{v}_2(t_1 = 25) = \overline{v}_1(t_1 = 25)\ ,\ \overline{v}_2'(t_1 = 25) = \overline{v}_1'(t_1 = 25)\ ,\ \overline{v}_2''(t_1 = 25) = \overline{v}_1''(t_1 = 25)\ .$$

In the case of the subinterval $I_3 = [50,\ 80]$, with $g_3 = 0$, we apply the same procedure described for $I_2 = [25,\ 50]$. The obtained OHPM solution $\overline{v}_3(t) = v_{3,0} + v_{3,1}$ is similar with Equation (44), depending on other optimally parameters.

The smoothing conditions are:

$$\overline{v}_3(t_2 = 50) = \overline{v}_2(t_2 = 50)\ ,\ \overline{v}_3'(t_2 = 50) = \overline{v}_2'(t_2 = 50)\ ,\ \overline{v}_3''(t_2 = 50) = \overline{v}_2''(t_2 = 50)\ .$$

4.2. Numerical Results via MOHPM Solutions

The comparison between MOHPM solutions v_{MOHPM} and the corresponding numerical ones for given initial conditions and for different values for 6 physical parameters a, b, c, d, e, f is quantitatively presented in detail in Tables 1–4.

Analogues, for the sets of physical parameters $\{a = 5.12, b = 0.84, c = 0.275, d = 1.65, e = 0.23, f = 1.24\}$, $\{a = 9.12, b = 0.84, c = 0.275, d = 1.65, e = 0.23, f = 1.24\}$ and $\{a = 17.35, b = 0.84, c = 0.275, d = 1.65, e = 0.23, f = 1.24\}$, respectively, MOHPM procedure could be applied using same operators (see the previous case) and three subintervals (as in Figure 1 by color curves).

Table 1. The numerical function $v_{numerical}$ for $x_{i0} = 0.25$, $y_{i0} = 0.5$, $z_{i0} = 1.5$, physical parameters $a = 2.096$, $b = 0.84$, $c = 0.275$, $d = 1.65$, $e = 0.23$, $f = 1.24$; $\bar{v}_{MOHPM}$ solution from Equation (7) using Equations (42), (44) and (A1)–(A3) and absolute residual values $\epsilon_v = |v_{numerical} - \bar{v}_{MOHPM}|$.

$t[s]$	$v_{numerical}$	$\bar{v}_{MOHPM}$	ϵ_v
0	1.9675	1.9674999999	2.6953×10^{-12}
4.9	0.0007246903	0.0007343748	9.6845×10^{-6}
9.8	0.0007548212	0.0007471019	7.7192×10^{-6}
14.7	0.0031470518	0.0031375659	9.4859×10^{-6}
19.6	0.0171881316	0.0171860083	2.1233×10^{-6}
24.5	0.1025576575	0.1025538940	3.7634×10^{-6}
25	0.1226928506	0.1226928606	9.9999×10^{-9}
29.9	0.4894132279	0.4894082654	4.9625×10^{-6}
34.8	0.1421869974	0.1421926453	5.6479×10^{-6}
39.7	0.1015678270	0.1015578887	9.9382×10^{-6}
44.6	0.1765077626	0.1765249589	1.7196×10^{-5}
49.5	0.2274595389	0.2274827496	2.3210×10^{-5}
50	0.2242436196	0.2242436296	9.9999×10^{-9}
55.9	0.1635299567	0.1635463752	1.6418×10^{-5}
61.8	0.1719745029	0.1719794558	4.9528×10^{-6}
67.7	0.1886226383	0.1886166392	5.9991×10^{-6}
73.6	0.1779317669	0.1779156827	1.6084×10^{-5}
79.5	0.1768300176	0.1768112112	1.8806×10^{-5}

Table 2. The numerical function $v_{numerical}$ for $x_{i0} = 0.25$, $y_{i0} = 0.5$, $z_{i0} = 1.5$, physical parameters $a = 17.35$, $b = 0.84$, $c = 0.275$, $d = 1.65$, $e = 0.23$, $f = 1.24$; $\bar{v}_{MOHPM}$ solution from Equation (7) using Equations (42), (44) and (A4)–(A6) and absolute residual values $\varepsilon_v = |v_{numerical} - \bar{v}_{MOHPM}|$.

$t[s]$	$v_{numerical}$	$\bar{v}_{MOHPM}$	ε_v
0	1.9675	1.9675000000000002	2.2204×10^{-16}
0.6	2.4162104775	2.4161744247	3.6052×10^{-5}
1.2	3.1061195892	3.1061882393	6.8650×10^{-5}
1.7	3.9694875168	3.9694409021	4.6614×10^{-5}
2	4.2994870305	4.2994871305	9.9999×10^{-8}
2.1	4.4726200822	4.4726190524	1.0297×10^{-6}
2.2	4.6511661102	4.6511595299	6.5802×10^{-6}
2.3	4.8350800394	4.8350643319	1.5707×10^{-5}
2.4	5.0242809392	5.0242561585	2.4780×10^{-5}
2.5	5.2186472454	5.2186173281	2.9917×10^{-5}
2.6	5.4180115926	5.4179830417	2.8550×10^{-5}
2.7	5.6221557512	5.6221353155	2.0435×10^{-5}
3	6.2602108416	6.2602108516	9.9998×10^{-9}
9.8	11.2496112759	11.2496139126	2.6366×10^{-6}
16.6	11.2253112998	11.2253131501	1.8502×10^{-6}
23.4	11.2251971066	11.2251940518	3.0548×10^{-6}
30.2	11.2251968132	11.2251967501	6.3089×10^{-8}
37	11.2251968128	11.2251968145	1.6327×10^{-9}

A qualitatively analysis of the MOHPM solutions regarding the influence of the physical parameter a is depicted in Figure 1. These MOHPM solutions describe heteroclinic orbits of the System (1) taking into account the Equations (6).

As the value of parameter a increases, the damped oscillation acquires an asymptotic behavior, the other physical parameters being fixed.

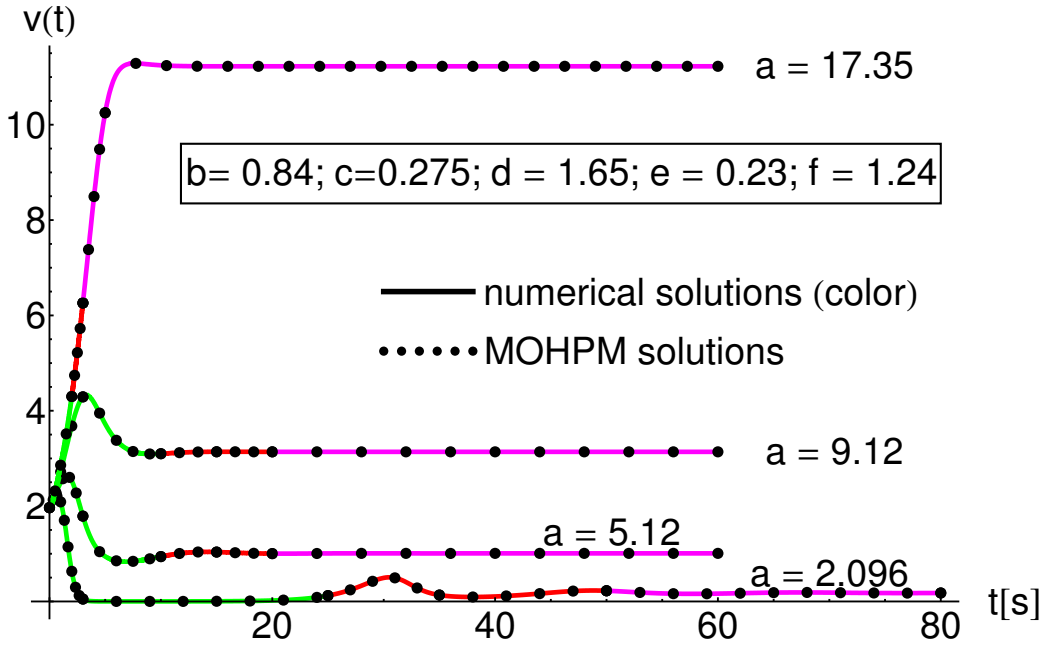


Figure 1. Effects of parameter a on MOHPM solution $\bar{v}_{MOHPM}$ (dotted curves) versus numerical ones (color) for: $x_{i0} = 0.25$, $y_{i0} = 0.5$, $z_{i0} = 1.5$, physical parameters: $a \in \{2.096,\ 5.12,\ 9.12,\ 17.35\}$, $b = 0.84$, $c = 0.275$, $d = 1.65$, $e = 0.23$, $f = 1.24$. The green color curve corresponds to the subinterval I_1; the red color curve corresponds to the subinterval I_2; the magenta color curve corresponds to the subinterval I_3.

Additionally, for initial data $x_{i0} = 0.25$, $y_{i0} = 0.5$, $z_{i0} = 1.5$ and physical parameters $a = 2.096$, $b = 0.84$, $c = 0.275$, $d = 1.65$, $e = 0.23$, $f = 1.24$ it can be seen that the limit

$$\lim_{t\to\infty}(\bar{x}_{MOHPM}(t), \bar{y}_{MOHPM}(t), \bar{z}_{MOHPM}(t)) = (0.1196183139,\ 0.6803159745,\ 0.4387316583) \approx$$
$$(0.1196152415,\ 0.6803134725,\ 0.4387220298) = \left(\frac{e}{f}\sqrt{\frac{ac}{bd}},\ \sqrt{\frac{ae}{bf}},\ \frac{a}{b}\sqrt{\frac{ce}{fd}}\right),$$

where $(\bar{x}_{MOHPM}(t), \bar{y}_{MOHPM}(t), \bar{z}_{MOHPM}(t))$ is obtained from Equation (6). Therefore, the functions set $(\bar{x}_{MOHPM}(t), \bar{y}_{MOHPM}(t), \bar{z}_{MOHPM}(t))$ describes a heteroclinic orbit for the System (1).

The magnitude of the residual function is shown in Figure 2 on $I_1 = [0,\ 25]$, Figure 3 on $I_1 = [25,\ 50]$, Figure 4 on $I_1 = [50,\ 80]$, and in each case has order 10^{-5}, for $a = 2.096$; $b = 0.84; c = 0.275; d = 1.65; e = 0.23; f = 1.24$. Thus, the accuracy of the MOHPM procedure is in a good agreement with the corresponding numerical ones.

A comparison for the original state $x(t)$ of the System (1) is shown in Figure 5 and Table 3 for explain the numerical validation in both situation: numerical and corresponding MOHPM result.

Table 3. The numerical function $x_{numerical}$ for $x_{i0} = 0.25$, $y_{i0} = 0.5$, $z_{i0} = 1.5$, physical parameters $a = 2.096$, $b = 0.84$, $c = 0.275$, $d = 1.65$, $e = 0.23$, $f = 1.24$; $\bar{x}_{MOHPM}$ solution of the System (1) using Equations (42), (44) and (A1)–(A3) and absolute residual values $\varepsilon_x = |x_{numerical} - \bar{x}_{MOHPM}|$.

$t[s]$	$x_{numerical}$	$\bar{x}_{MOHPM}$	ε_x
0	0.25	0.2500000000001474	1.4738×10^{-13}
4.9	0.0133829027	0.0136081850	2.2528×10^{-4}
9.8	0.0053583061	0.0058023876	4.4408×10^{-4}
14.7	0.0085145866	0.0091368368	6.2225×10^{-4}
19.6	0.0171979618	0.0172986645	1.0070×10^{-4}
24.5	0.0420908335	0.0421692351	7.8401×10^{-5}
25	0.0469233468	0.0469244810	1.1341×10^{-6}
29.9	0.1737794642	0.1737764045	3.0596×10^{-6}
34.8	0.1372048693	0.1372165964	1.1727×10^{-5}
39.7	0.0818970396	0.0818443638	5.2675×10^{-5}
44.6	0.1033321753	0.1033414825	9.3072×10^{-6}
49.5	0.1377996073	0.1378336875	3.4080×10^{-5}
50	0.1387309605	0.1387310836	1.2306×10^{-7}
55.9	0.1175481161	0.1175444427	3.6734×10^{-6}
61.8	0.1135901427	0.1136039543	1.3811×10^{-5}
67.7	0.1228793721	0.1228854664	6.0942×10^{-6}
73.6	0.1202953010	0.1202932793	2.0217×10^{-6}
79.5	0.1181018888	0.1180982809	3.6079×10^{-6}

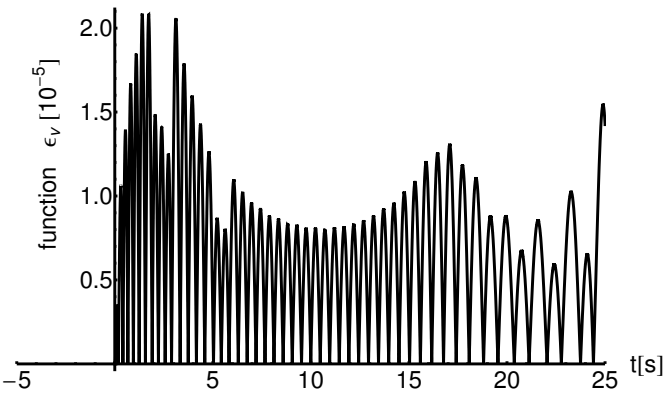


Figure 2. The residual function $\varepsilon_v(t) = |v_{numerical} - \bar{v}_{MOHPM}|$ on interval $I_1 = [0,\ 25]$ for $x_{i0} = 0.25$, $y_{i0} = 0.5$, $z_{i0} = 1.5$, physical parameters $a = 2.096$, $b = 0.84$, $c = 0.275$, $d = 1.65$, $e = 0.23$, $f = 1.24$.

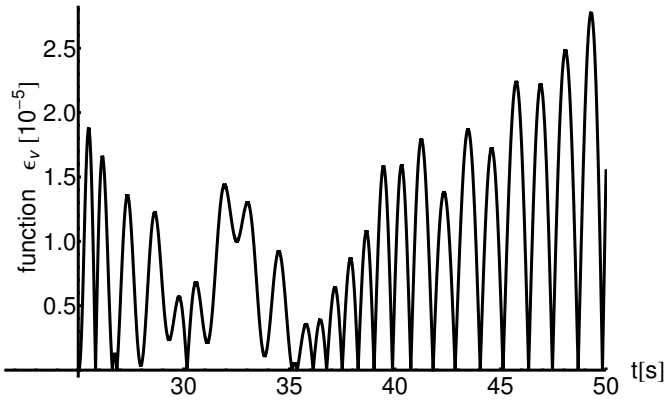


Figure 3. The residual function $\varepsilon_v(t) = |v_{numerical} - \bar{v}_{MOHPM}|$ on interval $I_2 = [25,\ 50]$ for $x_{i0} = 0.25$, $y_{i0} = 0.5$, $z_{i0} = 1.5$, physical parameters $a = 2.096$, $b = 0.84$, $c = 0.275$, $d = 1.65$, $e = 0.23$, $f = 1.24$.

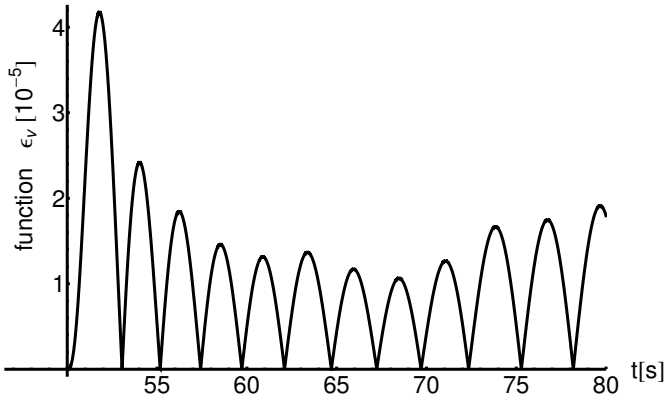


Figure 4. The residual function $\varepsilon_v(t) = |v_{numerical} - \bar{v}_{MOHPM}|$ on interval $I_3 = [50,\ 80]$ for $x_{i0} = 0.25$, $y_{i0} = 0.5$, $z_{i0} = 1.5$, physical parameters $a = 2.096$, $b = 0.84$, $c = 0.275$, $d = 1.65$, $e = 0.23$, $f = 1.24$.

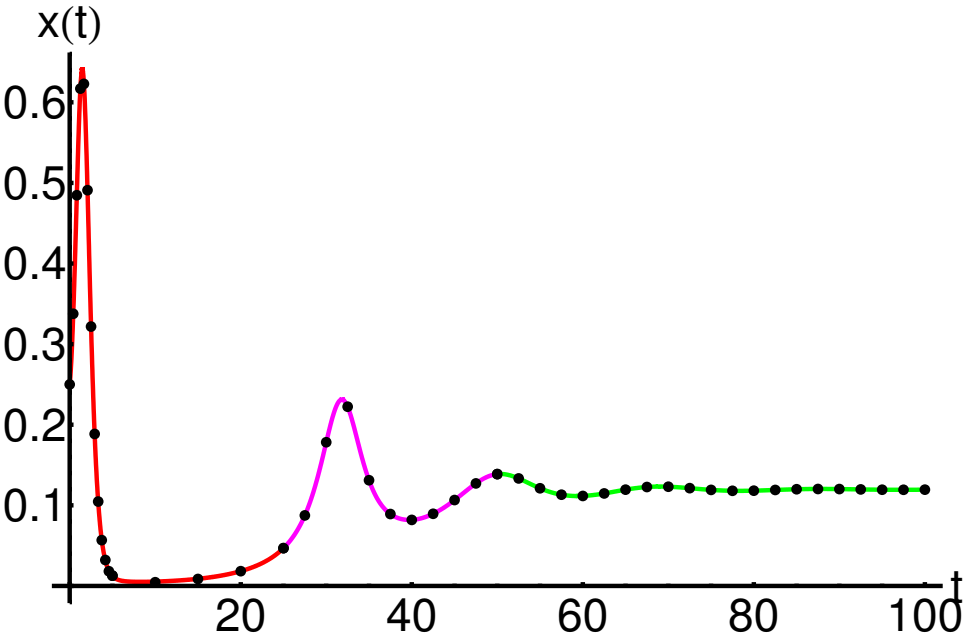


Figure 5. The MOHPM solution $\bar{x}_{MOHPM}$ (dotted curves) versus numerical ones (color) for the original state $x(t)$ when: $x_{i0} = 0.25$, $y_{i0} = 0.5$, $z_{i0} = 1.5$, physical parameters: $a = 2.096$, $b = 0.84$, $c = 0.275$, $d = 1.65$, $e = 0.23$, $f = 1.24$. The red color curve corresponds to the subinterval I_1; the magenta color curve corresponds to the subinterval I_2; the green color curve corresponds to the subinterval I_3.

The case of the almost periodical solutions using MOHPM.

Based on the Remark 1 we assume that the following conditions are satisfied:

$$c = \frac{bf}{3ae}\frac{-a^2+4ae-e^2}{a-e} > 0, 3c\frac{ae}{bf} + a - e > 0, a > e$$

and, therefore the matrix defined by Equation (3) admits one negative real eigenvalue and two complex conjugate eigenvalues (purely imaginary). For the physical parameters $a = 2.0$, $b = 1.05$, $c = \frac{bf}{3ae}\frac{-a^2+4ae-e^2}{a-e} = 0.22$, $d = 2.65$, $e = 0.6$, $f = 2.4$ the eigenvalues are $\lambda_1 \simeq -1.7142857142$, $\lambda_{2,3} \simeq \pm 0.5416025603\,\imath$, $\imath = \sqrt{-1}$.

The extended domain is assumed $I = [0,\ 40]$ and we split this into two subintervals $I_1 = [0,\ 20]$, $I_2 = [20,\ 40]$.

In what follows just we present the keys elements of the OHPM procedure for this case:

(a) For the first subinterval $I_1 = [t_0,\ t_1] = [0,\ 20]$, with $g_1 = 0$, the operators that appear in Equation (16) are:

$$\mathcal{L}_1[v(t)] = v''' + K_1^{(1)} v'' + (\omega_0^{(1)})^2 v' + K_1^{(1)}(\omega_0^{(1)})^2 v\,, \tag{45}$$

and

$$\mathcal{N}_1[v(t)] = \mathcal{N}[v(t)] - \left[v''' + K_1^{(1)} v'' + (\omega_0^{(1)})^2 v' + K_1^{(1)}(\omega_0^{(1)})^2 v\right]. \tag{46}$$

(b) The first-order OHPM solution $\overline{v}_1(t) = v_{1,0}(t) + v_{1,1}(t)$, is defined by Equation (23), with $v_{1,0}(t)$ solution of the Equation (22) taking into account the initial conditions from Equation (7):

$$v_{1,0}(t) = A_1^{(1)}\cos(\omega_0^{(1)} t) + B_1^{(1)}\sin(\omega_0^{(1)} t) + A_0^{(1)} e^{-K^{(1)}{}_1 t}\,. \tag{47}$$

The expression of operator $\mathcal{N}_1[v_{1,0}(t)]$ defined in Equation (29) becomes a linear combination of the functions $g_{1,k}(t)h_{1,k}(t)$ as in Equation (30), where:

$$g_{1,k}(t)h_{1,k}(t) \in \Big\{1\,,\ \cos(\omega_0^{(1)} t)\,,\ \sin(\omega_0^{(1)} t)\,,\ \cos(\omega_0^{(1)} t)e^{-K_1^{(1)} t}\,,\ \sin(\omega_0^{(1)} t)e^{-K_1^{(1)} t}\,,\ 1\cdot e^{-K_1^{(1)} t}\,,\ 1\cdot e^{-2K_1^{(1)} t}\,,\ 1\cdot e^{-4K_1^{(1)} t}\,,$$
$$\cos(2\omega_0^{(1)} t)\,,\ \sin(2\omega_0^{(1)} t)\,,\ \cos(3\omega_0^{(1)} t)e^{-3K_1^{(1)} t}\,,\ \sin(3\omega_0^{(1)} t)e^{-3K_1^{(1)} t}\,,\ \cos(2\omega_0^{(1)} t)e^{-2K_1^{(1)} t}\,,\ \sin(2\omega_0^{(1)} t)e^{-2K_1^{(1)} t}\Big\}\,, \tag{48}$$

and $K_{1,k}$ some real constants depending on $A_0^{(1)}$, $A_1^{(1)}$, $A_2^{(1)}$ and $\omega_0^{(1)}$. There are n = 14 elementary functions.

(c) We choose the auxiliary functions:

$\tilde{H}_{1,k}\left(t, g_{1,i}(t), C_{1,k_1}\right)$, $k = 1,\ 2, \ldots,\ n = 14$, for $j = 1$, as:

$$\tilde{H}_{1,1} = \tilde{B}_0\,, \quad \tilde{H}_{1,2} = \tilde{A}_1\cos(\omega_0^{(1)} t)\,, \quad \tilde{H}_{1,3} = \tilde{B}_1\sin(\omega_0^{(1)} t)\,,$$
$$\tilde{H}_{1,4} = \tilde{A}_0\,, \quad \tilde{H}_{1,5} = \tilde{A}_2\,, \quad \tilde{H}_{1,6} = \tilde{A}_3\,,$$
$$\tilde{H}_{1,7} = \sum_{i=1}^{N_{max}} \tilde{C}_i\cos((2i-1)\omega_0^{(1)} t)\,, \quad \tilde{H}_{1,8} = \sum_{i=1}^{N_{max}} \tilde{D}_i\sin((2i-1)\omega_0^{(1)} t)\,, \quad \tilde{H}_{1,9} = \sum_{i=1}^{N_{max1}} \tilde{E}_i\cos((2i)\omega_0^{(1)} t)\,,$$
$$\tilde{H}_{1,10} = \sum_{i=1}^{N_{max1}} \tilde{F}_i\sin((2i)\omega_0^{(1)} t)\,, \quad \tilde{H}_{1,11} = \sum_{i=1}^{2} \tilde{G}_i\cos((2i)\omega_0^{(1)} t)\,, \quad \tilde{H}_{1,12} = \sum_{i=1}^{2} \tilde{F}_i\sin((2i)\omega_0^{(1)} t)\,,$$
$$\tilde{H}_{1,13} = \sum_{i=1}^{2} \tilde{M}_i\cos(3(2i-1)\omega_0^{(1)} t)\,, \quad \tilde{H}_{1,14} = \sum_{i=1}^{2} \tilde{N}_i\sin(3(2i-1)\omega_0^{(1)} t)\,,$$

By a simple computation, the first approximation $v_{1,1}(t)$ defined in Equation (32), can be written as a linear combination of the above functions.

(d) The first-order approximate solution $\overline{v}_1(t)$, using OHPM method, is obtained by Equations (23), (32) and (47), for $j = 1$:

$$\begin{aligned}\overline{v}_1(t) = v_{1,0}(t) + v_{1,1}(t) = B_0^{(1)} + A_1^{(1)}\cos(\omega_0^{(1)}t + B_1^{(1)}\sin(\omega_0^{(1)}t) + A_0^{(1)}e^{-K_1^{(1)}t} + \\ A_2^{(1)}e^{-2K_1^{(1)}t} + A_3^{(1)}e^{-4K_1^{(1)}t} + \sum_{i=1}^{N_{max}}\left(C_i^{(1)}\cos((2i-1)\omega_0^{(1)}t) + D_i^{(1)}\sin((2i-1)\omega_0^{(1)}t)\right)e^{-K_1^{(1)}t} + \\ \sum_{i=1}^{N_{max1}}\left(E_i^{(1)}\cos((2i)\omega_0^{(1)}t) + F_i^{(1)}\sin((2i)\omega_0^{(1)}t)\right)e^{-2K_1^{(1)}t} + \sum_{i=1}^{2}\left(G_i^{(1)}\cos((2i)\omega_0^{(1)}t) + H_i^{(1)}\sin((2i)\omega_0^{(1)}t)\right) + \\ \sum_{i=1}^{2}\left(M_i^{(1)}\cos((2i-1)\omega_0^{(1)}t) + N_i^{(1)}\sin((2i-1)\omega_0^{(1)}t)\right)e^{-3K^{(1)}t},\end{aligned} \tag{49}$$

where all real parameters depending on $K_{1,k}$ will be optimally computed, via the least squares method (see Appendix A, Equation (A8)).

Following the same procedure as for subinterval $I_1 = [0,\ 20]$, for the second subinterval $I_2 = [20,\ 40]$, the first-order approximate solution $\overline{v}_2(t)$ is obtained as in Equation (49) and this depends on other optimally parameters (see Appendix A, Equation (A9)).

The effect of physical parameter d in the case of almost periodical solutions is represented in the Figure 6.

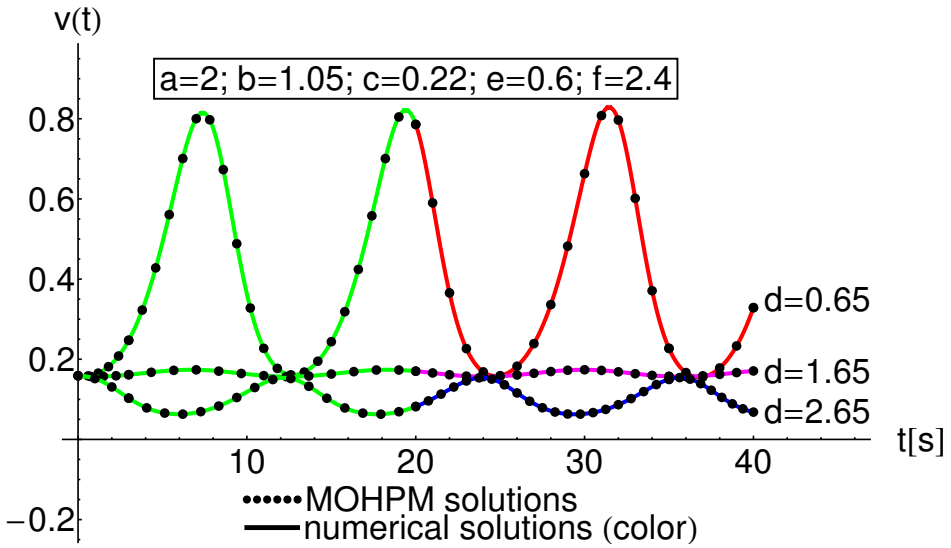


Figure 6. Effects of parameter d on MOHPM solution $\overline{v}_{MOHPM}$ (dotted curves) versus numerical ones (color) for: $x_{i0} = 0.125$, $y_{i0} = 0.69$, $z_{i0} = 0.34$, physical parameters: $d \in \{0.65,\ 1.65,\ 2.65\}$, $a = 2.0$, $b = 1.05$, $c = \frac{bf}{3ae}\frac{-a^2+4ae-e^2}{a-e} = 0.22$, $e = 0.6$, $f = 2.4$. The green color curve corresponds to the subinterval I_1; the red color curve corresponds to the subinterval I_2 for $d = 0.65$; the magenta color curve corresponds to the subinterval I_2 for $d = 1.65$; the blue color curve corresponds to the subinterval I_2 for $d = 2.65$.

The residual function $\varepsilon_v(t) = |v_{numerical} - \overline{v}_{MOHPM}|$ has order of magnitude 10^{-6} and it is shown in the Figures 7 and 8 for physical parameters $a = 2.0$, $b = 1.05$, $c = \frac{bf}{3ae}\frac{-a^2+4ae-e^2}{a-e} = 0.22$, $d = 2.65$, $e = 0.6$, $f = 2.4$, while the corresponding almost periodical orbit is graphically presented in the Figure 9.

Table 4. The numerical function $v_{numerical}$ for $x_{i0} = 0.125$, $y_{i0} = 0.69$, $z_{i0} = 0.34$, physical parameters $a = 2.0$, $b = 1.05$, $c = \frac{bf}{3ae}\frac{-a^2+4ae-e^2}{a-e} = 0.22$, $d = 2.65$, $e = 0.6$, $f = 2.4$; $\overline{v}_{MOHPM}$ solution from Equation (7) using Equations (49), (A8) and (A9) and absolute residual values $\varepsilon_v = |v_{numerical} - \overline{v}_{MOHPM}|$.

$t[s]$	$v_{numerical}$	$\overline{v}_{MOHPM}$	ε_v
0	0.15888	0.1588800000	1.9456×10^{-14}
2.4375	0.1187524899	0.1187524573	3.2591×10^{-8}
4.875	0.0678184429	0.0678185737	1.3083×10^{-7}

Table 4. *Cont.*

$t[s]$	$v_{numerical}$	$\bar{v}_{MOHPM}$	ε_v
7.3125	0.0696975695	0.0696972470	3.2255×10^{-7}
9.75	0.1125389953	0.1125392659	2.7063×10^{-7}
12.1875	0.1537404659	0.1537405829	1.1704×10^{-7}
14.625	0.1057830147	0.1057825814	4.3332×10^{-7}
17.0625	0.0643773397	0.0643773976	5.7888×10^{-8}
19.5	0.0747636189	0.0747633878	2.3112×10^{-7}
20	0.0820929641	0.0820929641	4.5519×10^{-15}
22.4375	0.1349480361	0.1349446374	3.3987×10^{-6}
24.875	0.1446155704	0.1446137026	1.8677×10^{-6}
27.3125	0.0825196642	0.0825209570	1.2927×10^{-6}
29.75	0.0630636897	0.0630665080	2.8182×10^{-6}
32.1875	0.0901104995	0.0901134282	2.9286×10^{-6}
34.625	0.1441908219	0.1441922906	1.4686×10^{-6}
37.0625	0.1345770785	0.1345750340	2.0445×10^{-6}
39.5	0.0744082421	0.0744120335	3.7914×10^{-6}

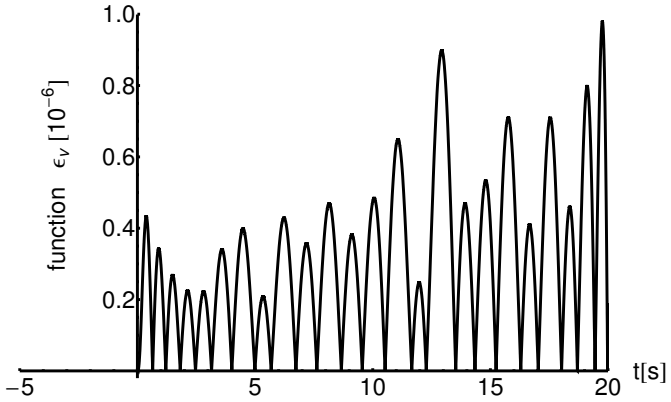


Figure 7. The residual function $\varepsilon_v(t) = |v_{numerical} - \bar{v}_{MOHPM}|$ on interval $I_1 = [0, 20]$ for $x_{i0} = 0.125$, $y_{i0} = 0.69$, $z_{i0} = 0.34$, physical parameters $a = 2.0$, $b = 1.05$, $c = \frac{bf}{3ae}\frac{-a^2+4ae-e^2}{a-e} = 0.22$, $d = 2.65$, $e = 0.6$, $f = 2.4$.

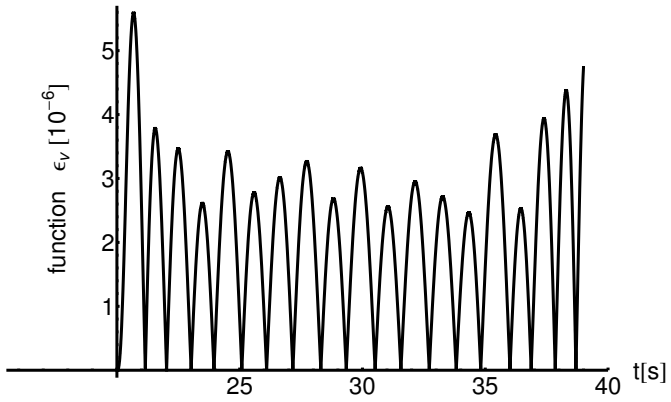


Figure 8. The residual function $\varepsilon_v(t) = |v_{numerical} - \bar{v}_{MOHPM}|$ on interval $I_2 = [20, 40]$ for $x_{i0} = 0.125$, $y_{i0} = 0.69$, $z_{i0} = 0.34$, physical parameters $a = 2.0$, $b = 1.05$, $c = \frac{bf}{3ae}\frac{-a^2+4ae-e^2}{a-e} = 0.22$, $d = 2.65$, $e = 0.6$, $f = 2.4$.

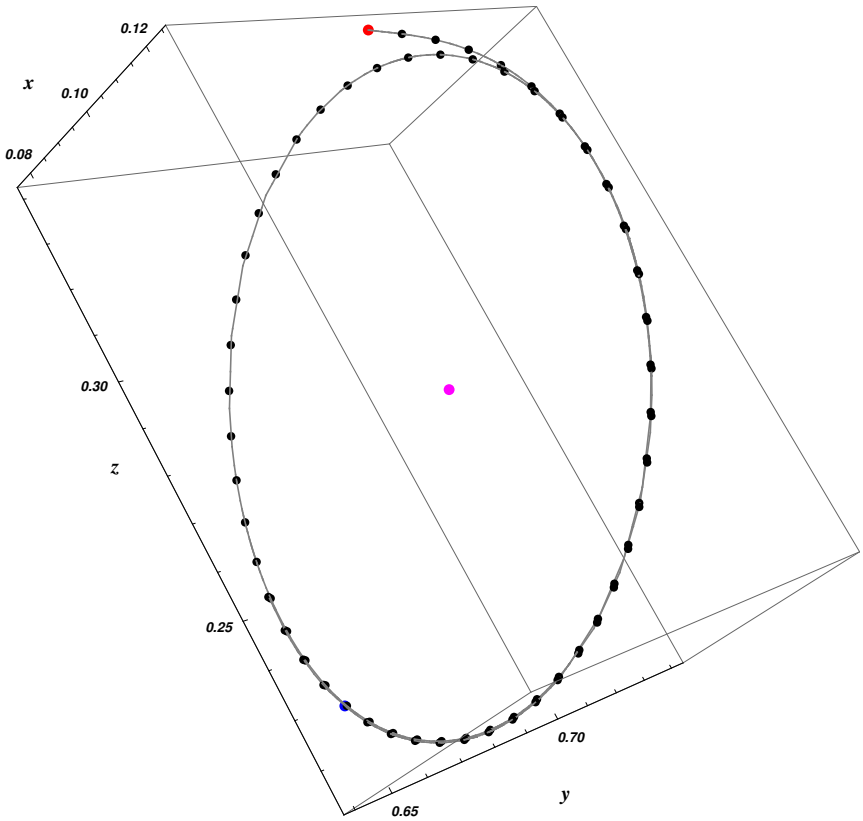


Figure 9. Almost periodical orbit $(x(t), y(t), z(t))$ (gray curve for numerical results) versus $(\overline{x}_{MOHPM}(t), \overline{y}_{MOHPM}(t), \overline{z}_{MOHPM}(t))$ (dotted black curve for MOHPM results), for initial conditions $x_{i0} = 0.125$, $y_{i0} = 0.69$, $z_{i0} = 0.34$ (red point), physical parameters $a = 2.0$, $b = 1.05$, $c = \frac{bf}{3ae}\frac{-a^2+4ae-e^2}{a-e} = 0.22$, $d = 2.65$, $e = 0.6$, $f = 2.4$; equilibrium point $\left(\frac{e}{f}\sqrt{\frac{ac}{bd}}, \sqrt{\frac{ae}{bf}}, \frac{a}{b}\sqrt{\frac{ec}{fd}}\right)$ (magenta point) and the point $(x(19), y(19), z(19))$ (blue point), respectively.

4.3. Comparison Between MOHPM and OHPM Results

In this subsection is presented a comparative analysis between OHPM solution and corresponding numerical solution in two situations: (a) using an extended index number N_{max} and (b) for a small index number N_{max}.

The linear and nonlinear operators will be the same as Equations (38) and (39), choosing the initial extended interval $I = [0,\ 80]$. The obtained OHPM solution is analogous as in Equation (42) depending on other optimal parameters (see Appendix A, Equation (A7)).

In both situations can be seen that the accuracy of the OHPM method decreases. These behaviors are exposed in Figures 10 and 11 for one extended index number N_{max}, and Figure 12 and Figure 13, respectively, using a small index number N_{max}.

The solution presented below is to explain the overfitting phenomenon when applying OHPM over the entire interval $[0,\ 80]$.

In Figure 11 is plotted the magnitude of the residual function $\varepsilon_v(t)$ for OHMP solution $\overline{v}_{OHPM}$ when the optimal parameters are computed using extended interval $[0,\ 80]$. The magnitude of the residual function has order 10^{-3} by comparison with the corresponding ones using MOHPM method, smaller with two orders of magnitude, 10^{-5}.

Applying OHPM technique on an extended computational domain, but using a small index number N_{max}, the precision of OHPM-solution $\overline{v}_{OHPM}$ decreases as in the accompanying Figures 12 and 13. The magnitude of the residual function has order 10^{-2} by comparison with corresponding ones using MOHPM method, as mentioned in the previous case.

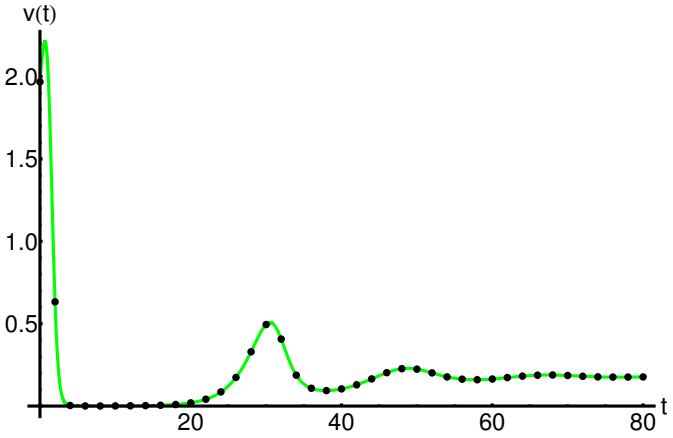


Figure 10. Comparative profiles between OHPM solution $\overline{v}_{OHPM}$ using Equations (42) and (A7); numerical ones (color) for: $x_{i0} = 0.25$, $y_{i0} = 0.5$, $z_{i0} = 1.5$, physical parameters: $a = 2.096$, $b = 0.84$, $c = 0.275$, $d = 1.65$, $e = 0.23$, $f = 1.24$.

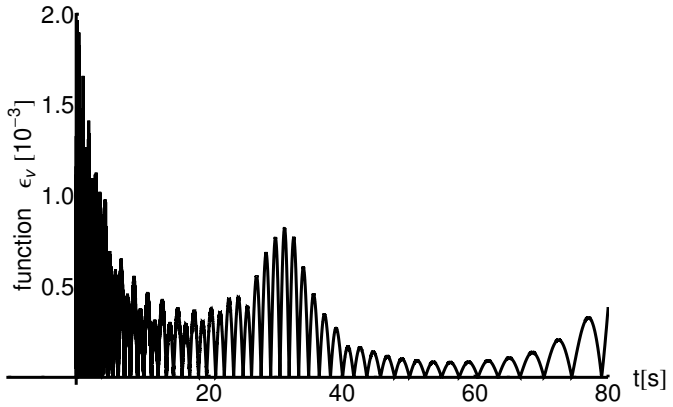


Figure 11. The residual function $\varepsilon_v(t) = |v_{numerical} - \bar{v}_{OHPM}|$ when $N_{max} = 20$, $N_1 = 10$ (the optimal parameters computed using extended interval $[0,\ 80]$) for $x_{i0} = 0.25$, $y_{i0} = 0.5$, $z_{i0} = 1.5$, physical parameters $a = 2.096$, $b = 0.84$, $c = 0.275$, $d = 1.65$, $e = 0.23$, $f = 1.24$.

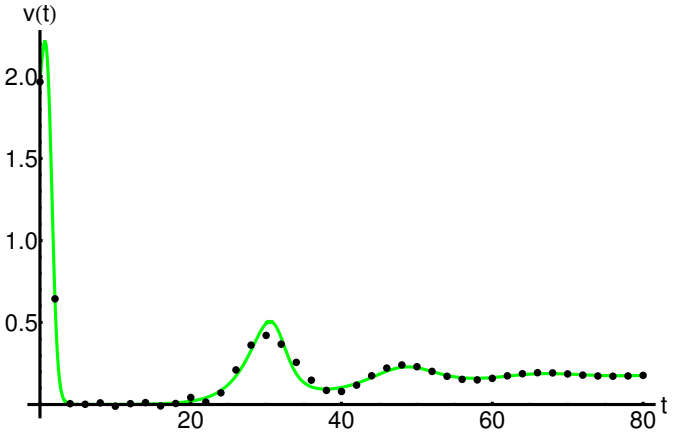


Figure 12. Comparative profiles between OHPM solution $(\overline{v}_{OHPM})$ using Equations (42) and (A7) for a small index number $N_{max} = 5$; numerical ones (color) for: $x_{i0} = 0.25$, $y_{i0} = 0.5$, $z_{i0} = 1.5$, physical parameters: $a = 2.096$, $b = 0.84$, $c = 0.275$, $d = 1.65$, $e = 0.23$, $f = 1.24$.

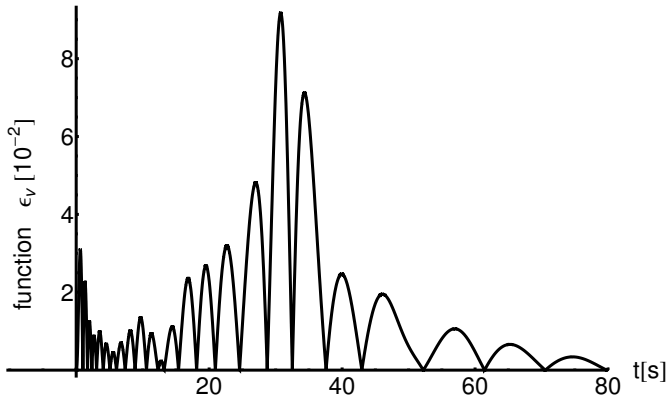


Figure 13. The residual function $\varepsilon_v(t) = |v_{numerical} - \bar{v}_{OHPM}|$ when $N_{max} = 5$, $N_1 = 2$ (the optimal parameters computed using extended interval $[0,\ 80]$) for $x_{i0} = 0.25$, $y_{i0} = 0.5$, $z_{i0} = 1.5$, physical parameters $a = 2.096$, $b = 0.84$, $c = 0.275$, $d = 1.65$, $e = 0.23$, $f = 1.24$.

4.4. Qualitatively Analysis of Errors

Some statistical tests for numerical solutions to deterministic systems have been proposed for a long time (see for example Hansen [34] or Den Haan et al. [35] or monographies of King et al. [36] or of Ding et al. [37]). Our investigation somewhat follows well-known studies for regression methods or information extraction from signals (see for example the monography of Spagnolini [38]). In fact, the used tests certify that the residual values are purely random and no analytical, i.e., deterministic, expression can be extracted. These residual values are only the result of numerical errors coming from approximation and truncation of real numbers and of the limitations of numerical methods for strongly nonlinear systems.

A qualitative analysis of errors is performed in the same manner as in [39,40], following the same steps but using statistical tests appropriate to the present data.

The primary challenge in analyzing more dynamic systems lies in the fact that the true values, or exact solutions, are often unknown. To approximate solutions, researchers rely on observations or data derived from physical phenomena, numerical solutions, or simulations. The discrepancies that arise between these approximations and numerical results (often derived from computational methods) are frequently referred to as "errors." However, a more suitable term in this context is "residuals." Performing a qualitative analysis of these residuals becomes an essential step, as it provides insights into the adequacy of the model or method used.

In statistics and optimization, "errors" are defined as the unobservable theoretical differences between observed values and the true model or exact solution. On the other hand, "residuals" are the observable differences between observed values and the predicted or estimated values derived from a sample model. Put simply, errors are inherently random and unmeasurable, whereas residuals are calculable and serve as proxies to estimate these underlying errors.

The concept of residuals has been discussed in seminal works, such as the one by Cox et al. [41] where residuals were given a general definition.

Numerical solutions, which play a critical role in many scientific applications, inherently come with limitations. They generate approximate, non-analytical results that can be computationally intensive, demand specialized expertise, and may suffer from issues such as instability or lack of convergence. These solutions often rely on complex discretization methods, which might struggle to accurately represent sharp discontinuities or material interfaces. Additionally, numerical methods typically involve truncation of real numbers, introducing further approximations.

Given these limitations, a qualitative analysis of residuals becomes a vital tool. This non-numerical diagnostic technique helps evaluate the performance of a model or approximation. Specifically, such an analysis aims to verify that residuals exhibit behavior akin to randomness with no discernible patterns or periodicity thereby implying that the approximation is reliable. The most utilized methods for residual analysis focus on three key aspects:

1. "Constant Mean and Variance": Residuals should have a constant mean value, which, in most cases, is close to zero. Equally important is ensuring constant variance of the residuals; any variability in variance (known as heteroscedasticity) can signal inadequacies in the model.

2. "Lack of Correlation": Residuals should not demonstrate correlation or autocorrelation. This ensures there are no recurring patterns or periodic behaviors in the data series and indicates that the chosen approximation is a valid representation of the system's dynamics.

3. "Distribution Shape": The empirical distribution of residuals should closely resemble a well-understood theoretical probability distribution, typically a normal (Gaussian) distribution.

There are numerous statistical tests available to evaluate these properties. Modern statistical software like R (version 4.5.0) or RStudio provides robust tools free of charge for conducting such analysis effectively.

In addition to statistical tests, simple visualizations can also offer immediate insights into the behavior and distribution of residuals. Examples include basic two-dimensional plots and histograms, which allow researchers to identify trends, patterns, and deviations more intuitively.

All computations required for these analysis in this study were performed using R software (version 4.5.0). This software offers extensive packages tailored for generating both statistical tests and graphical representations, making it an indispensable tool for such evaluations.

4.5. Graphical Representations

We split our data in five groups (the length of series is 100) i.e., $[1, 20]$, $[21, 40]$, $[41, 60]$, $[61, 80]$ and $[81, 100]$.

Graphical representations are depicted in Figure 14 for series of residuals and in Figure 15 for histogram of the residuals, respectively.

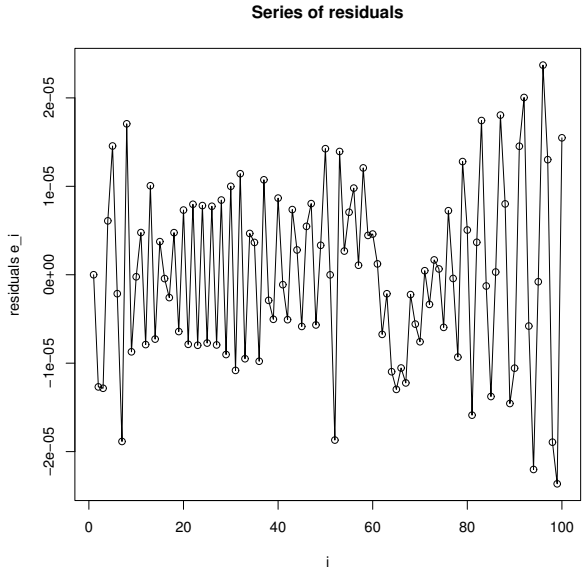


Figure 14. Series of residuals.

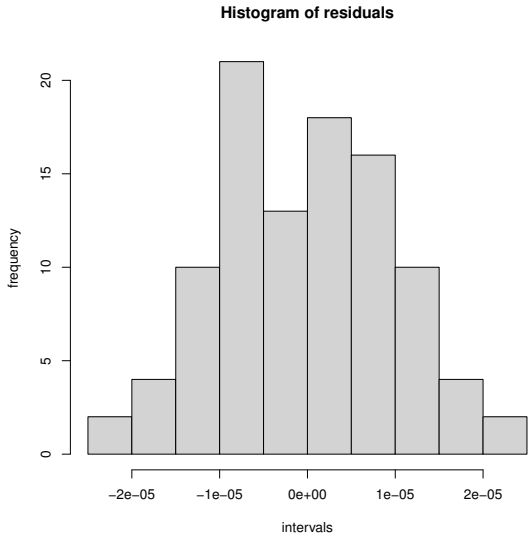


Figure 15. Histogram for the residuals.

4.6. Study of Heteroscedasticity

Results for our example:

- First, the boxplot graph is represented in Figure 16:

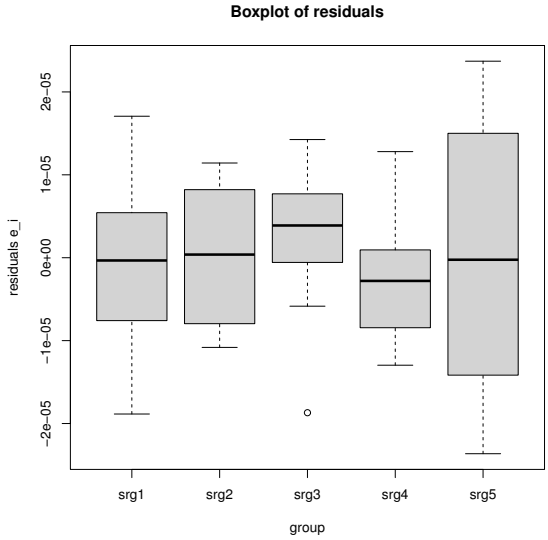


Figure 16. Box-plot for residuals. The White circle represents one singular point belongs to subgroup sgr3.

- Second, the statistical mean value, median value and, respectively, the standard deviation are shown in Tables 5, 6 and 7, respectively:

Table 5. Mean value of groups.

Subgroup	sg1	sg2	sg3	sg4	sg5
mean	-5.845235×10^{-7}	1.289427×10^{-7}	3.026934×10^{-6}	-3.045879×10^{-6}	3.517300×10^{-7}

Table 6. Standard deviation of groups.

Subgroup	sg1	sg2	sg3	sg4	sg5
st.deviation	9.383352×10^{-6}	8.516013×10^{-6}	7.835072×10^{-6}	6.835083×10^{-6}	1.537773×10^{-5}

Table 7. Median value of groups.

Subgroup	sg1	sg2	sg3	sg4	sg5
median	-3.314324×10^{-7}	3.793317×10^{-7}	3.889660×10^{-6}	-2.798158×10^{-6}	-2.415459×10^{-7}

We observe some differences between mean and median values, i.e., there exist an asymmetry and therefore we compute the skewness for each groups in the Table 8:

Table 8. Skewness for groups.

Subgroup	sg1	sg2	sg3	sg4	sg5
skewness	0.01305165	0.01209538	−0.85071022	0.43780820	−0.06023775

and we can see some nonzero values for skewness at the group 4 and respective group 5 (moderate skew), hence it is possible to have a non-normal distribution of the residuals (see test for normality from below). Also, the presence of some significant asymmetry can affect the results of some classical statistical test for homoscedasticity (see for example Yonar et al. [42] or Wang et al. [43])

The Brown-Forsythe test is a robust statistical method for evaluating equality of variances across three or more independent groups. It acts as a modification of Levene's test, utilizing deviations from the group median rather than the mean, which makes it less sensitive to non-normal data and better at handling skewed distributions or outliers (see for example [44]).

- The Brown-Forsythe test R
  Null Hypothesis (H_0): All group variances are equal.
  Alternative Hypothesis (H_a): At least two group variances are different.
  Results from R-software (version 4.5.0):
  F = 0.93629, num df = 4.000, denom df = 64.746, p-value = 0.4487
  Detailed,
  Brown-Forsythe Test (alpha = 0.05)
  dependent var: sr
  grouping var: srg
  F = 0.9362895
  num df = 4
  denom df = 64.74583
  p-value = 0.44865
  Result: Difference is not statistically significant.
  Because, the p-value > 0.05, then the decision is "fails to reject the null hypothesis", i.e., "The assumption of equal variances (homoscedasticity) holds true".

4.7. Study of Autocorrelation

Results for our example:

- Durbin-Watson test
  Null Hypothesis (H_0): There is no first-order autocorrelation in the residuals.
  Alternative Hypothesis (H_a): First-order autocorrelation exists.
  As a simple remark for the statistical decision, a p-value below 0.05 indicates significant autocorrelation, allowing rejection of the null hypothesis that residuals are uncorrelated. Also, some common interpretations in the case of the auto-correlation presence:
  $DW \approx 2$: Residuals are likely independent (no autocorrelation).

$DW < 2$: Suggests positive autocorrelation, common in time-series data.
$DW > 2$: Suggests negative autocorrelation
Results from the R-software:
DW = 2.3064, p-value = 0.8744 alternative hypothesis: true autocorrelation is greater than 0
We have that the p-value < 0.05, hence, the statistical decision is "fails to reject the null hypothesis"

4.8. Study of Normality

- Shapiro-Wilk test
  Results for our data:
  W = 0.99237, p-value = 0.8473
  In this case, the p-value < 0.05, then a decision can be "it is false to reject H_0", i.e., "data is normal".
- Jarque-Bera test Because, some moderate skew is observed, we perform a more adequate test for our data, i.e., Jarque-Bera test (see [45]).
  Results from R-software:
  X-squared = 1.1449, df = 2, p-value = 0.5642
  The p-value > 0.05, hence, the statistical decision is "it is false to reject the null hypothesis of normality".

Moreover, the Kruskal–Wallis test is a nonparametric or distribution-free, is performed. The hypotheses for the Kruskal–Wallis test are as follows:

- Null hypothesis: the samples (groups) are drawn from identical populations.
- Alternative hypothesis: at least one sample (group) comes from a population that differs from the others.

Output from R for our data:
Kruskal–Wallis chi-squared = 4.922, df = 4, p-value = 0.2954
Hence, the p-value > 0.05 and then the statistical decision is "it is false to reject the null hypothesis".

5. Conclusions

By applying the Multistage Optimal Homotopy Perturbation Method (MOHPM), this work successfully determines the closed-form solutions for a six-parameter dynamical system. The precision of this novel analytical approach is rigorously validated against numerical solutions using both graphical and tabular representations. Critically, the MOHPM demonstrates superior accuracy, producing residuals on the order of 10^{-5} compared to the 10^{-3} order of the traditional OHPM. Complemented by a thorough qualitative error analysis including heteroscedasticity, autocorrelation, and normality test, these results underscore the method's potential for analyzing complex dynamical systems in engineering and natural sciences.

Author Contributions: Conceptualization, R.-D.E., R.N. and N.P.; methodology, R.N. and N.P.; software, R.-D.E., R.N. and N.P.; validation, R.-D.E., R.N. and N.P.; formal analysis, R.-D.E., R.N. and N.P.; investigation, R.-D.E., R.N., R.B. and N.P.; writing—original draft preparation, R.-D.E., R.N., R.B. and N.P.; writing—review and editing, R.-D.E., R.N., R.B. and N.P.; visualization, R.-D.E., R.N., R.B. and N.P.; supervision, R.N. and N.P. All authors have read and agreed to the published version of the manuscript.

Funding: This research received no external funding.

Data Availability Statement: The original contributions presented in this study are included in the article. Further inquiries can be directed to the corresponding author.

Acknowledgments: The author N.P. would like to acknowledge the contribution of the COST Action CA21169, supported by COST (European Cooperation in Science and Technology).

Conflicts of Interest: The authors declare no conflicts of interest.

Appendix A

The optimally parameters for approximate solution via MOHPM procedure, $\bar{v}_{MOHPM}$ obtained by the classical least squares method are given in this Appendix A by the Wolfram Mathematica software 9.0 using the "NMinimize" package (for calculus of the optimally parameters) and "NDSolve" package (to compute the numerical solutions by forth-order Runge-Kutta method), respectively.

A division of the interval $[j+a,\ j+b]$ containing N_1 sampling points is a set denoted by

$$\mathcal{M}_j(a,b,N_1) = \{i_1 \ \big|\ i_1 = j+a : h_1 : j+b\}\ ,$$

with $h_1 = \frac{b-a}{N_1}$.

Example A1. *$\bar{v}_{MOHPM}$ is a MOHPM solution of the Equation (7) for the initial conditions $x_{i0} = 0.25$, $y_{i0} = 0.5$, $z_{i0} = 1.5$, physical parameters: $a = 2.096$, $b = 0.84$, $c = 0.275$, $d = 1.65$, $e = 0.23$, $f = 1.24$ and index $N_{max} = 20$, $N_{max1} = 10$.*

For interval $I_1 = [0,\ 25]$ (nonuniform behavior) the set of sampling points is chosen as

$$\mathcal{S}_1 = \cup_{j=0}^{2}\mathcal{M}_j(0,1,10) \cup \cup_{j=3}^{10}\mathcal{M}_j(0,1,5) \cup \cup_{j=11}^{25}\mathcal{M}_j(0,0.9999,5)\ .$$

Using the formula given by Equation (34) and the set of sampling points $\mathcal{S}_1$, the parameters from Equation (42) are:

$$\begin{array}{lll}
A_0^{(1)} = 16300.1272980455\ , & A_1^{(1)} = -41.2703105656\ , & A_2^{(1)} = -15709.7222008157\ , \\
C_0^{(1)} = 1.0881954689\ , & \tilde{T}_1^{(1)} = -4.3049545228\ , & \tilde{T}_2^{(1)} = 7.8045992156\ , \\
\tilde{T}_3^{(1)} = 1833.5690060931\ , & K^{(1)} = 0.4977899723\ , & K_1^{(1)} = 0.2051922783\ , \\
\omega_0^{(1)} = 0.1659421508\ , & D_1^{(1)} = -43.6375058468\ , & D_2^{(1)} = -8.4551093738\ , \\
D_3^{(1)} = -4.9396146998\ , & D_4^{(1)} = -9.8060453384\ , & D_5^{(1)} = -8.1807408549\ , \\
D_6^{(1)} = -8.5680287929\ , & D_7^{(1)} = -8.1681248018\ , & D_8^{(1)} = -5.4052198203\ , \\
D_9^{(1)} = -2.6930478926\ , & D_{10}^{(1)} = -1.3646119034\ , & D_{11}^{(1)} = 2.9504544210\ , \\
D_{12}^{(1)} = 1.6709723183\ , & D_{13}^{(1)} = 0.7907392806\ , & D_{14}^{(1)} = 0.3226798982\ , \\
D_{15}^{(1)} = 0.0101817948\ , & D_{16}^{(1)} = -0.1761649182\ , & D_{17}^{(1)} = -0.2000914252\ , \\
D_{18}^{(1)} = -0.0866623095\ , & D_{19}^{(1)} = 0.0162931617\ , & D_{20}^{(1)} = 0.0137880277\ , \\
E_1^{(1)} = 7.5394122177\ , & E_2^{(1)} = -26.8688669500\ , & E_3^{(1)} = -23.7692241061\ , \\
E_4^{(1)} = -55.8559810145\ , & E_5^{(1)} = -35.1886958508\ , & E_6^{(1)} = 3.2347137056\ , \\
E_7^{(1)} = 7.0576771262\ , & E_8^{(1)} = -7.9766808233\ , & E_9^{(1)} = 8.0822482887\ , \\
E_{10}^{(1)} = 3.4036024339\ , & E_{11}^{(1)} = 2.1643836985\ , & E_{12}^{(1)} = -0.2175887423\ , \\
E_{13}^{(1)} = -0.5116726347\ , & E_{14}^{(1)} = -0.5191894094\ , & E_{15}^{(1)} = -0.4233877597\ , \\
E_{16}^{(1)} = -0.2400221164\ , & E_{17}^{(1)} = -0.0296827316\ , & E_{18}^{(1)} = 0.085887807\ , \\
E_{19}^{(1)} = 0.0534672481\ , & E_{20}^{(1)} = 6.2306 \times 10^{-6}\ , & F_1^{(1)} = -447.9871609468\ , \\
F_2^{(1)} = -17.7898822984\ , & F_3^{(1)} = 9.6546241418\ , & F_4^{(1)} = 3.6954409342\ , \\
F_5^{(1)} = -1.8608316760\ , & F_6^{(1)} = -0.5839285968\ , & F_7^{(1)} = 0.9592105775\ , \\
F_8^{(1)} = -0.5622625584\ , & F_9^{(1)} = 0.0604246822\ , & F_{10}^{(1)} = 0.0972426833\ , \\
G_1^{(1)} = -878.6612013912\ , & G_2^{(1)} = -66.5130512467\ , & G_3^{(1)} = -10.4322901661\ , \\
G_4^{(1)} = 2.6916810031\ , & G_5^{(1)} = 1.5267014739\ , & G_6^{(1)} = -1.0780115384\ , \\
G_7^{(1)} = 0.0388932771\ , & G_8^{(1)} = 0.4006968253\ , & G_9^{(1)} = -0.2727668580\ , \\
G_{10}^{(1)} = 0.1250685571\ ; & & \\
\text{the RMSE test:} & 1.4901 \times 10^{-8}\ ; &
\end{array} \tag{A1}$$

For interval $I_2 = [25,\ 50]$ (uniform behavior), $N_{max} = 10$, $N_{max1} = 5$ the set of sampling points is proposed as $\mathcal{S}_2 = \cup_{j=25}^{50}\mathcal{M}_j(0,1,10)$.

By means of the formula given by Equation (34) and the set $\mathcal{S}_2$, the parameters from Equation (44) are:

$$\begin{array}{lll}
A_0^{(2)} = 684.6496650284\,, & A_1^{(2)} = 481.9992287380\,, & A_2^{(2)} = -18068.9780174455\,, \\
C_0^{(2)} = 0.1794224992\,, & \tilde{T}_1^{(2)} = -15.4360435682\,, & \tilde{T}_2^{(2)} = -13.4162206346\,, \\
K_1^{(2)} = 0.1706003242\,, & \omega_0^{(2)} = 0.2178505718\,, & D_1^{(2)} = 12.8057822611\,, \\
D_2^{(2)} = -2.4485420144\,, & D_3^{(2)} = 0.1974254512\,, & D_4^{(2)} = -0.0511005721\,, \\
D_5^{(2)} = 0.0446132315\,, & D_6^{(2)} = 0.0015486536\,, & D_7^{(2)} = 0.0009354817\,, \\
D_8^{(2)} = 0.0014239323\,, & D_9^{(2)} = -0.0019842187\,, & D_{10}^{(2)} = 0.0001687860\,, \\
E_1^{(2)} = 25.2696427246\,, & E_2^{(2)} = -1.8559302702\,, & E_3^{(2)} = 0.3895392792\,, \\
E_4^{(2)} = -0.1411219236\,, & E_5^{(2)} = 0.0145495964\,, & E_6^{(2)} = 0.0207307358\,, \\
E_7^{(2)} = 0.0042884663\,, & E_8^{(2)} = -0.0028939145\,, & E_9^{(2)} = -0.0012797717\,, \\
E_{10}^{(2)} = 0.0017119735\,, & F_1^{(2)} = -12888.4213507909\,, & F_2^{(2)} = 1837.3798467118\,, \\
F_3^{(2)} = -996.1230623368\,, & F_4^{(2)} = 158.1944416469\,, & F_5^{(2)} = 2.7585543551\,, \\
G_1^{(2)} = -13741.7087382381\,, & G_2^{(2)} = 1246.3690977889\,, & G_3^{(2)} = -261.5077194602\,, \\
G_4^{(2)} = -99.4334626113\,, & G_5^{(2)} = 1.5613240618\,; & \\
\text{the RMSE test:} & 3.6818 \times 10^{-8}\,; &
\end{array} \tag{A2}$$

For interval $I_3 = [50,\ 80]$ (uniform behavior), $N_{max} = 10$, $N_{max1} = 5$ the set of sampling points is assumed as $\mathcal{S}_3 = \cup_{j=50}^{80}\mathcal{M}_j(0,1,10)$.

Using the Equation (34) and the set $\mathcal{S}_3$, the parameters from Equation (44) become:

$$\begin{array}{lll}
A_0^{(3)} = 135.0891810424\,, & A_1^{(3)} = 30.1243525983\,, & A_2^{(3)} = -27062.5024494501\,, \\
\tilde{T}_1^{(3)} = -1.4524919919\,, & \tilde{T}_2^{(3)} = -0.2994201943\,, & K_1^{(3)} = 0.1086473366\,, \\
\omega_0^{(3)} = 0.1017032638\,, & D_1^{(3)} = 6.1087230729\,, & D_2^{(3)} = 0.2377201190\,, \\
D_3^{(3)} = -0.3700507472\,, & D_4^{(3)} = 0.0237448128\,, & D_5^{(3)} = 0.0243484353\,, \\
D_6^{(3)} = -0.4589473440\,, & D_7^{(3)} = -0.5809792070\,, & D_8^{(3)} = -0.0528505175\,, \\
D_9^{(3)} = -0.0284401015\,, & D_{10}^{(3)} = 0.3396109732\,, & E_1^{(3)} = 26.5517800772\,, \\
E_2^{(3)} = 2.4994358558\,, & E_3^{(3)} = 0.1377646848\,, & E_4^{(3)} = 0.1076982625\,, \\
E_5^{(3)} = -0.0375843360\,, & E_6^{(3)} = -0.5256412087\,, & E_7^{(3)} = -0.8424738018\,, \\
E_8^{(3)} = -0.0711244277\,, & E_9^{(3)} = 0.1653332074\,, & E_{10}^{(3)} = -0.2881804513\,, \\
F_1^{(3)} = -24719.6987041350\,, & F_2^{(3)} = 2624.5927429377\,, & F_3^{(3)} = 1806.9241863883\,, \\
F_4^{(3)} = 0.5108275987\,, & F_5^{(3)} = -0.48246798716\,, & G_1^{(3)} = -26391.5162250041\,, \\
G_2^{(3)} = -11699.9438584968\,, & G_3^{(3)} = -51.0222378466\,, & G_4^{(3)} = 0.2068323332\,, \\
G_5^{(3)} = -0.0601815730\,; & & \\
\text{the RMSE test:} & 9.7795 \times 10^{-7}\,. &
\end{array} \tag{A3}$$

Example A2. *$\bar{v}_{MOHPM}$ is a semi-analytical solution of the Equation (7) for the initial conditions $x_{i0} = 0.25$, $y_{i0} = 0.5$, $z_{i0} = 1.5$, physical parameters: $a = 17.35$, $b = 0.84$, $c = 0.275$, $d = 1.65$, $e = 0.23$, $f = 1.24$ and index $N_{max} = 20$, $N_{max1} = 10$.*

For interval $I_1 = [0,\ 2]$ (nonuniform behavior) the set of sampling points is chosen as

$$\mathcal{S}_1 = \cup_{j=0}^{1}\mathcal{M}_j(0,1,10) \cup \cup_{j=1}^{2}\mathcal{M}_j(0,1,5)\,.$$

Using the formula given by Equation (34) and the set $\mathcal{S}_1$, the parameters from Equation (42) are:

$$
\begin{array}{lll}
A_0^{(1)} = -6.9543429964\,, & A_1^{(1)} = 0.1663372780\,, & A_2^{(1)} = -1.1168855631\,,\\
C_0^{(1)} = 0.2637656837\,, & \tilde{T}_1^{(1)} = -0.1873379656\,, & \tilde{T}_2^{(1)} = 24.6484828590\,,\\
\tilde{T}_3^{(1)} = 2.9666604700\,, & K^{(1)} = 14.1233416392\,, & K_1^{(1)} = 0.1912000330\,,\\
\omega_0^{(1)} = 0.0444783787\,, & D_1^{(1)} = -0.4284729132\,, & D_2^{(1)} = 0.9792084798\,,\\
D_3^{(1)} = -0.4600480239\,, & D_4^{(1)} = 0.3221908977\,, & D_5^{(1)} = 0.6628444176\,,\\
D_6^{(1)} = -0.3055351696\,, & D_7^{(1)} = 0.1806340783\,, & D_8^{(1)} = -0.3525599379\,,\\
D_9^{(1)} = 0.1687863769\,, & D_{10}^{(1)} = 0.0449164572\,, & D_{11}^{(1)} = 1.2513621570\,,\\
D_{12}^{(1)} = -0.4599441873\,, & D_{13}^{(1)} = 1.2199689832\,, & D_{14}^{(1)} = 1.4488498223\,,\\
D_{15}^{(1)} = 0.2275086457\,, & D_{16}^{(1)} = 0.6931809521\,, & D_{17}^{(1)} = -0.5628939717\,,\\
D_{18}^{(1)} = 0.6472246905\,, & D_{19}^{(1)} = 1.1301576157\,, & D_{20}^{(1)} = 0.4570940779\,,\\
E_1^{(1)} = 0.4438209212\,, & E_2^{(1)} = 0.0431118322\,, & E_3^{(1)} = 0.9488269142\,,\\
E_4^{(1)} = 0.6536732890\,, & E_5^{(1)} = 0.5449193558\,, & E_6^{(1)} = -1.2860298895\,,\\
E_7^{(1)} = -0.6759451563\,, & E_8^{(1)} = -0.9571678729\,, & E_9^{(1)} = -0.6391279808\,,\\
E_{10}^{(1)} = -0.2333444137\,, & E_{11}^{(1)} = 0.4540574689\,, & E_{12}^{(1)} = -0.3382172178\,,\\
E_{13}^{(1)} = 0.7297708481\,, & E_{14}^{(1)} = 1.3221845377\,, & E_{15}^{(1)} = -0.6773057407\,,\\
E_{16}^{(1)} = 0.1564344451\,, & E_{17}^{(1)} = -0.3224996776\,, & E_{18}^{(1)} = -0.8952172002\,,\\
E_{19}^{(1)} = -0.3914294024\,, & E_{20}^{(1)} = 0.9279569530\,, & F_1^{(1)} = 0.7029958824\,,\\
F_2^{(1)} = 0.5926527270\,, & F_3^{(1)} = -0.4622499939\,, & F_4^{(1)} = -1.0200876091\,,\\
F_5^{(1)} = -0.2409683885\,, & F_6^{(1)} = -0.2043356210\,, & F_7^{(1)} = -0.5110573085\,,\\
F_8^{(1)} = 0.5826375106\,, & F_9^{(1)} = 0.8061138357\,, & F_{10}^{(1)} = 0.5309511142\,,\\
G_1^{(1)} = 0.6636990926\,, & G_2^{(1)} = 0.8862468265\,, & G_3^{(1)} = 0.0360520500\,,\\
G_4^{(1)} = -0.4321067155\,, & G_5^{(1)} = -0.8624545267\,, & G_6^{(1)} = 0.2761581342\,,\\
G_7^{(1)} = 0.7094374963\,, & G_8^{(1)} = 0.3462996778\,, & G_9^{(1)} = -0.0863609613\,,\\
G_{10}^{(1)} = 0.7825345323\,; & & \\
\text{the RMSE test:} & 2.4718 \times 10^{-7}\,; &
\end{array}
\tag{A4}
$$

For interval $I_2 = [2,\ 3]$ (uniform behavior), $N_{max} = 5$, $N_{max1} = 2$ the set of sampling points is proposed as $\mathcal{S}_2 = \cup_{j=2}^{3}\mathcal{M}_j(0, 1, 15)$.

By means of the formula given by Equation (34) and the set $\mathcal{S}_2$, the parameters from Equation (44) are:

$$
\begin{array}{lll}
A_0^{(2)} = 0.5511360533\,, & A_1^{(2)} = 0.2647253722\,, & A_2^{(2)} = 0.4226147842\,,\\
C_0^{(2)} = 0.9249348854\,, & \tilde{T}_1^{(2)} = 1.0062559287\,, & \tilde{T}_2^{(2)} = -0.0518964400\,,\\
H_3^{(2)} = 0.1701947204\,, & K^{(2)} = 0.0137661739\,, & K_1^{(2)} = 0.0021825581\,,\\
\omega_0^{(2)} = 0.1188361325\,, & D_1^{(2)} = 0.6289696856\,, & D_2^{(2)} = 0.6105499573\,,\\
D_3^{(2)} = -1.7305403641\,, & D_4^{(2)} = -1.4459591932\,, & D_5^{(2)} = 0.7482689580\,,\\
E_1^{(2)} = -2.3383742364\,, & E_2^{(2)} = 0.0816304076\,, & E_3^{(2)} = -0.3571462854\,,\\
E_4^{(2)} = -0.9815298618\,, & E_5^{(2)} = 0.7885631284\,, & F_1^{(2)} = -0.1141911164\,,\\
F_2^{(2)} = -0.8158333752\,, & G_1^{(2)} = -0.9005536396\,, & G_2^{(2)} = -0.0724617972\,;\\
\text{the RMSE test:} & 4.8839 \times 10^{-9}\,; &
\end{array}
\tag{A5}
$$

Related to interval $I_3 = [3,\ 20]$ (uniform behavior), $N_{max} = 5$, $N_{max1} = 2$ we consider the set of sampling points by $\mathcal{S}_3 = \cup_{j=3}^{20}\mathcal{M}_j(0, 1, 10)$.

Using the Equation (34) and the set $\mathcal{S}_3$, the convergence-control parameters for $\bar{v}_{MOHPM}$ that appear in Equations (44) become:

$$\begin{array}{lll}
A_0^{(3)} = -27.5794650993\,, & A_1^{(3)} = 3.2162888764\,, & A_2^{(3)} = -312.5319902232\,, \\
\tilde{T}_1^{(3)} = 1.4689110674\,, & \tilde{T}_2^{(3)} = -0.6424091694\,, & K_1^{(3)} = 0.6370157394\,, \\
\omega_0^{(3)} = 0.3176709050\,, & D_1^{(3)} = 0.1489491098\,, & D_2^{(3)} = 0.0733716638\,, \\
D_3^{(3)} = 0.0382871727\,, & D_4^{(3)} = -0.0251024609\,, & D_5^{(3)} = 0.0053527593\,, \\
E_1^{(3)} = 0.2423156439\,, & E_2^{(3)} = 0.0442015550\,, & E_3^{(3)} = -0.0359442654\,, \\
E_4^{(3)} = 0.0060951071\,, & E_5^{(3)} = -0.0069014273\,, & F_1^{(3)} = 196.2570627757\,, \\
F_2^{(3)} = -43.9856580627\,, & F_3^{(3)} = 14.5958900375\,, & G_1^{(3)} = 214.0797593841\,, \\
G_2^{(3)} = 14.1908717940\,, & G_3^{(3)} = 10.8970882111\,; & \\
\text{the RMSE test:} & 7.5595 \times 10^{-9}\,. &
\end{array} \tag{A6}$$

Example A3. *$\bar{v}_{OHPM}$ is a semi-analytical solution of the Equation (7) using OHPM method for the initial conditions $x_{i0} = 0.25$, $y_{i0} = 0.5$, $z_{i0} = 1.5$, physical parameters: $a = 2.096$, $b = 0.84$, $c = 0.275$, $d = 1.65$, $e = 0.23$, $f = 1.24$ and index $N_{max} = 20$, $N_{max1} = 10$.*

For comparison with OHPM results using an extended domain $I = [0,\ 80]$ we propose the set of sampling points by

$$\mathcal{S} = \cup_{j=0}^{2}\mathcal{M}_j(0,1,10) \cup \cup_{j=3}^{10}\mathcal{M}_j(0,1,5) \cup \cup_{j=11}^{40}\mathcal{M}_j(0,0.9999,5) \cup \cup_{j=41}^{80}\mathcal{M}_j(0,0.9999,5)\,.$$

The convergence-control parameters for $\bar{v}_{OHPM}$ that appear in Equation (42) are optimally identified using the set $\mathcal{S}$ and formula given by Equation (34) by:

$$\begin{array}{lll}
A_0 = -1.8220328398152253 \times 10^{12}\,, & A_1 = 1.0713408608943607 \times 10^{11}\,, & A_2 = 4.750615754311887 \times 10^{12}, \\
C_0 = 0.1794224992115676\,, & \tilde{T}_1 = 4421.258082476955\,, & \tilde{T}_2 = -697.0932419343876, \\
\tilde{T}_3 = -4.418365752809414 \times 10^{11}\,, & K = 0.46553836530676823\,, & K_1 = 0.2159293545425615, \\
\omega_0 = 0.05084318409773785\,, & D_1 = 4.0867189487489716 \times 10^{11}\,, & D_2 = -3.2163383180588022 \times 10^{12}, \\
D_3 = 9.819018242523556 \times 10^{11}\,, & D_4 = -2.703942788508915 \times 10^{11}\,, & D_5 = -3.927317018636189 \times 10^{10}, \\
D_6 = 6.585876291561328 \times 10^{10}\,, & D_7 = -1.194397453467586 \times 10^{10}\,, & D_8 = -3.573234151165819 \times 10^{10}, \\
D_9 = 1.6855012667636951 \times 10^{10}\,, & D_{10} = 3.571461509711797 \times 10^{10}\,, & D_{11} = -2.0272409232124207 \times 10^{10}, \\
D_{12} = -6.159043639882631 \times 10^{9}\,, & D_{13} = 3.2424027398806624 \times 10^{9}\,, & D_{14} = 1.5522819882477105 \times 10^{9}, \\
D_{15} = -4.1064943361751044 \times 10^{8}\,, & D_{16} = -2.354182508450287 \times 10^{8}\,, & D_{17} = 4.663276703443951 \times 10^{7}, \\
D_{18} = 1.2622351535866234 \times 10^{7}\,, & D_{19} = -2.1808360185874854 \times 10^{6}\,, & D_{20} = -53411.02575950957, \\
E_1 = -1.863502295601897 \times 10^{11}\,, & E_2 = 3.886903754052551 \times 10^{11}\,, & E_3 = 2.0887775595822382 \times 10^{11}, \\
E_4 = -1.2386069633536719 \times 10^{11}\,, & E_5 = -1.3030722602759192 \times 10^{11}\,, & E_6 = -2.569054656228809 \times 10^{11}, \\
E_7 = 2.0676057016726593 \times 10^{10}\,, & E_8 = 1.4424730644195505 \times 10^{11}\,, & E_9 = -2.0025451916806778 \times 10^{10}, \\
E_{10} = -1.6045665927951302 \times 10^{10}\,, & E_{11} = -1.5722739624248693 \times 10^{10}\,, & E_{12} = 8.752748642992504 \times 10^{9}, \\
E_{13} = 3.1645208358015823 \times 10^{9}\,, & E_{14} = -1.1659177813545341 \times 10^{9}\,, & E_{15} = -6.625213913285055 \times 10^{8}, \\
E_{16} = 1.4307933711928725 \times 10^{8}\,, & E_{17} = 6.516094177738971 \times 10^{7}\,, & E_{18} = -1.2348147079631621 \times 10^{7}, \\
E_{19} = -1.4063580213172124 \times 10^{6}\,, & E_{20} = 182194.93993264262\,, & F_1 = -8.360754396052637 \times 10^{11}, \\
F_2 = -1.3453184586310153 \times 10^{11}\,, & F_3 = -6.009849753822255 \times 10^{9}\,, & F_4 = 1.6596771912925278 \times 10^{10}, \\
F_5 = 1.1543029191238274 \times 10^{10}\,, & F_6 = 1.8479500446787806 \times 10^{9}\,, & F_7 = -1.666398551835027 \times 10^{9}, \\
F_8 = -6.044212229956186 \times 10^{8}\,, & F_9 = 7.23447502181478 \times 10^{7}\,, & F_{10} = 1.6646803264996251 \times 10^{7}, \\
G_1 = 1.5552775555342075 \times 10^{11}\,, & G_2 = -1.1397658995122963 \times 10^{11}\,, & G_3 = -5.838006790144577 \times 10^{10}, \\
G_4 = -1.8719606234696426 \times 10^{10}\,, & G_5 = 1.3488214662326405 \times 10^{9}\,, & G_6 = 4.967091653997535 \times 10^{9}, \\
G_7 = 1.4217349025968642 \times 10^{9}\,, & G_8 = -4.316193630103389 \times 10^{8}\,, & G_9 = -1.553469352666415 \times 10^{8}, \\
G_{10} = 4.516690130136028 \times 10^{6}\,; & & \\
\text{the RMSE test:} & 3.7102 \times 10^{-5}\,. &
\end{array} \tag{A7}$$

Example A4. *Based on the Remark 1 here is considered the case of the almost periodical solution when $c = \frac{bf}{3ae}\frac{-a^2+4ae-e^2}{a-e}$, $a > e$. $\bar{v}_{MOHPM}$ is a MOHPM solution of the Equation (7) for the initial conditions $x_{i0} = 0.125$, $y_{i0} = 0.69$, $z_{i0} = 0.34$, physical parameters: $a = 2.0$, $b = 1.05$, $c = \frac{bf}{3ae}\frac{-a^2+4ae-e^2}{a-e} = 0.22$, $d = 2.65$, $e = 0.6$, $f = 2.4$ and index $N_{max} = 10$, $N_{max1} = 8$.*

For interval $I_1 = [0,\ 20]$ (nonuniform behavior) the set of sampling points is chosen as

$$\mathcal{S}_1 = \cup_{j=0}^{2}\mathcal{M}_j(0,1,5) \cup \cup_{j=3}^{10}\mathcal{M}_j(0,1,2) \cup \cup_{j=11}^{20}\mathcal{M}_j(0,0.9999,2)\ .$$

Using the formula given by Equation (34) and the set of sampling points $\mathcal{S}_1$, the parameters from Equation (49) are:

$$\begin{array}{lll}
A_1^{(1)} = -3.2723403026\,, & A_2^{(1)} = -0.1573822930\,, & A_3^{(1)} = 4.2873954060\,, \\
B_0^{(1)} = -20.2380002697\,, & K_1^{(1)} = 0.2365941099\,, & \omega_0 = 0.1213728316\,, \\
C_1^{(1)} = 42.1749243243\,, & C_2^{(1)} = 98.7655489694\,, & C_3^{(1)} = -9.2278238871\,, \\
C_4^{(1)} = 13.2529730780\,, & C_5^{(1)} = 12.2233242953\,, & C_6^{(1)} = 7.8500286333\,, \\
C_7^{(1)} = 3.3228563711\,, & C_8^{(1)} = 0.6491178644\,, & C_9^{(1)} = 0.0007040055\,, \\
C_{10}^{(1)} = 0.0021566862\,, & D_1^{(1)} = 1.2221180959\,, & D_2^{(1)} = -0.2151013799\,, \\
D_3^{(1)} = 2.9722324654\,, & D_4^{(1)} = 0.3624169831\,, & D_5^{(1)} = -3.6760915607\,, \\
D_6^{(1)} = -0.0203666331\,, & D_7^{(1)} = 0.9074965056\,, & D_8^{(1)} = 0.9183694090\,, \\
D_9^{(1)} = 0.1261882460\,, & D_{10}^{(1)} = 0.0059895115\,, & E_1^{(1)} = -1.0675774840\,, \\
E_2^{(1)} = 2.5102493718\,, & E_3^{(1)} = 3.6808496454\,, & E_4^{(1)} = -11.1814991827\,, \\
E_5^{(1)} = -29.4391602842\,, & E_6^{(1)} = 3.2746032959\,, & E_7^{(1)} = -2.0780358254\,, \\
E_8^{(1)} = 1.4083690175\,, & ,F_1^{(1)} = 1.0169827531\,, & F_2^{(1)} = 0.7451683981\,, \\
F_3^{(1)} = -0.3561435247\,, & ,F_4^{(1)} = -1.1051667407\,, & F_5^{(1)} = -0.9092502199\,, \\
F_6^{(1)} = -1.3724990395\,, & F_7^{(1)} = -8.7823050158\,, & F_8^{(1)} = 1.0395185006\,, \\
G_1^{(1)} = 20.4061820536\,, & G_2^{(1)} = -3.0130064637\,, & H_1^{(1)} = 19.1067080918\,, \\
H_2^{(1)} = 1.7910428146\,, & M_1^{(1)} = -0.6797155783\,, & M_2^{(1)} = -2.8450143021\,, \\
N_1^{(1)} = -16.8821049729\,, & N_2^{(1)} = 2.0412224210\,; & \\
\text{the RMSE test:} & 5.0522 \times 10^{-12}\,; &
\end{array} \tag{A8}$$

For interval $I_1 = [20,\ 40]$ (uniform behavior) the set of sampling points is

$$\mathcal{S}_1 = \cup_{j=0}^{20}\mathcal{M}_j(0,1,2)\ .$$

Using the formula given by Equation (34) and the set of sampling points $\mathcal{S}_1$, the parameters from Equation (49) are:

$$\begin{array}{lll}
A_0^{(2)} = -0.9913391272\,, & A_1^{(2)} = -1.0515124441\,, & A_2^{(2)} = -0.9833138583\,, \\
A_3^{(2)} = -0.9690216100\,, & B_1^{(2)} = -0.4746095990\,, & K_1^{(2)} = 0.0013297404\,, \\
\omega_0^{(2)} = 0.1163226680\,, & C_1^{(2)} = -1.0506031923\,, & C_2^{(2)} = -0.7639988270\,, \\
C_3^{(2)} = -1.4752531021\,, & C_4^{(2)} = -0.7408592101\,, & C_5^{(2)} = -0.9743637128\,, \\
C_6^{(2)} = -0.8605461633\,, & C_7^{(2)} = -0.9495038530\,, & C_8^{(2)} = -0.0866383270\,, \\
C_9^{(2)} = 0.0177004404\,, & C_{10}^{(2)} = -0.0009555192\,, & D_1^{(2)} = -0.4931392561\,, \\
D_2^{(2)} = -1.1445343581\,, & D_3^{(2)} = -1.2579752400\,, & D_4^{(2)} = -0.6263922237\,, \\
D_5^{(2)} = -0.4256971472\,, & D_6^{(2)} = -0.7047264055\,, & D_7^{(2)} = -1.0496146228\,, \\
D_8^{(2)} = -0.5799390880\,, & D_9^{(2)} = -0.0334657353\,, & D_{10}^{(2)} = 0.0004288305\,, \\
E_1^{(2)} = -1.1284688715\,, & E_2^{(2)} = -0.7142820929\,, & E_3^{(2)} = -1.1579261035\,, \\
E_4^{(2)} = -0.8735786271\,, & E_5^{(2)} = -0.8848111514\,, & E_6^{(2)} = -1.0949403196\,, \\
E_7^{(2)} = -0.4999660251\,, & ,E_8^{(2)} = 0.0397951660\,, & F_1^{(2)} = -1.2036974120\,, \\
F_2^{(2)} = -0.7717125203\,, & F_3^{(2)} = -1.1903058454\,, & F_4^{(2)} = -0.2515220653\,, \\
F_5^{(2)} = -0.7041885105\,, & F_6^{(2)} = -0.8552911153\,, & F_7^{(2)} = -1.0197852545\,, \\
F_8^{(2)} = -0.2094681212\,, & G_1^{(2)} = -1.1262979377\,, & G_2^{(2)} = -0.6908960167\,, \\
H_1^{(2)} = -1.2117843445\,, & H_2^{(2)} = -0.7692095420\,, & M_1^{(2)} = -1.0488946925\,, \\
M_2^{(2)} = -0.7767971225\,, & N_1^{(2)} = -0.5278947010\,, & N_2^{(2)} = -1.1395855438\,; \\
\text{the RMSE test:} & 2.3807 \times 10^{-10}\ . &
\end{array} \tag{A9}$$

References

1. Khattar, D.; Agrawal, N.; Sirohi, M. Qualitative Analysis of a New 6D Hyper–Chaotic System via Bifurcation, the Poincaré Notion, and Its Circuit Implementation. *Indian J. Phys.* **2023**, *98*, 259–273. [CrossRef]
2. Chowdhury, M.; Razali, N.; Asrar, W.; Majid, Z. The Multistage Homotopy Perturbation Method for Solving Hyperchaotic Chen System. *J. Phys. Conf. Ser.* **2017**, *949*, 012005. [CrossRef]
3. Lorenz, E.N. Deterministic Nonperiodic Flow. *J. Atmos. Sci.* **1963**, *20*, 130–141. [CrossRef]
4. Zhang, M.; Han, Q. Dynamic analysis of an autonomous chaotic system with cubic nonlinearity. *Optik* **2016**, *127*, 4315–4319. [CrossRef]
5. Saeed, H.; Ali, A.; Menzer, R.; Potclean, A.; Arora, H. New Family of Multi-Step Iterative Methods Based on Homotopy Perturbation Technique for Solving Nonlinear Equations. *Mathematics* **2023**, *11*, 2603. [CrossRef]
6. Wang, H.; Ke, G.; Pan, J.; Su, Q. Modeling, Dynamical Analysis and Numerical Simulation of a New 3D Cubic Lorenz-Like System. *Sci. Rep.* **2023**, *13*, 6671. [CrossRef] [PubMed]
7. Lazureanu, C. On the Hamilton–Poisson realizations of the integrable deformations of the Maxwell-Bloch equations. *Comptes Rendus Math.* **2017**, *355*, 596–600. [CrossRef]
8. Lazureanu, C.; Hedrea, C.; Petrisor, C. On a deformed version of the two-disk dynamo system. *Appl. Math.* **2021**, *66*, 345–372. [CrossRef]
9. Lazureanu, C.; Cho, J. On a family of Hamilton–Poisson Jerk System. *Mathematics* **2024**, *12*, 1260. [CrossRef]
10. Biggs, R.; Remsing, C.C. Quadratic Hamilton–Poisson Systems in Three Dimensions: Equivalence, Stability, and Integration. *Acta Appl. Math.* **2017**, *148*, 1–59. [CrossRef]
11. Gholamin, P.; Sheikhani, A.H.R. A new three-dimensional chaotic system: Dynamical properties and simulation. *Chin. J. Phys.* **2017**, *55*, 1300–1309. [CrossRef]
12. Xu, M.; Shi, S.; Huang, K. On the integrable stretch-twist-fold flow: Bi-Hamiltonian structures and global dynamics. *J. Math. Phys.* **2024**, *65*, 022704. [CrossRef]
13. Bao, J.; Yang, Q. A new method to find homoclinic and heteroclinic orbits. *Appl. Math. Comput.* **2011**, *217*, 6526–6540. [CrossRef]
14. El–Dessoky, M.M.; Yassen, M.T.; Saleh, E.; Aly, E.S. Existence of heteroclinic and homoclinic orbits in two different chaotic dynamical systems. *Appl. Math. Comput.* **2012**, *218*, 11859–11870. [CrossRef]
15. Li, Z.; Liu, X.; Tian, Y. Existence of homoclinic orbits in three-dimensional piecewise linear forced oscillator systems. *Bull. Sci. Math.* **2026**, *209*, 103804. [CrossRef]
16. Harko, T.; Lobo, F.S.N.; Mak, M.K. Exact analytical solutions of the Susceptible-Infected-Recovered (SIR) epidemic model and of the SIR model with equal death and birth rates. *Appl. Math. Comput.* **2014**, *236*, 184–194. [CrossRef]
17. Puta, M. Integrability and geometric prequantization of the Maxwell-Bloch equations. *Bull. Sci. Math.* **1998**, *122*, 243–250. [CrossRef]
18. Olvera, D.; Elías-Zúñiga, A. Enhanced Multistage Homotopy Perturbation Method: Approximate Solutions of Nonlinear Dynamic Systems. *Abstr. Appl. Anal.* **2014**, *2014*, 1–12. [CrossRef]
19. He, J.-H. Homotopy Perturbation Technique. *Comput. Methods Appl. Mech. Eng.* **1999**, *178*, 257–262. [CrossRef]
20. He, J.-H. Homotopy Perturbation Method: A New Nonlinear Analytical Technique. *Appl. Math. Comput.* **2003**, *135*, 73–79. [CrossRef]
21. He, J.-H. New interpretation of homotopy perturbation method. *Int. J. Mod. Phys. B* **2006**, *20*, 2561–2568. [CrossRef]
22. Chowdhury, M.; Hashim, I.; Momani, S. The Multistage Homotopy-Perturbation Method: A Powerful Scheme for Handling the Lorenz System. *Chaos Solitons Fractals* **2009**, *40*, 1929–1937. [CrossRef]
23. Chowdhury, M.; Hashim, I.; Momani, S.; Rahman, M. Application of multistage homotopy perturbation method to the chaotic Genesio system. *Abstr. Appl. Anal.* **2012**, *10*, 974293. [CrossRef]
24. Chowdhury, M.; Razali, N.; Asrar, W.; Rahman, M. The Multistage Homotopy Perturbation Method for Solving Chaotic and Hyperchaotic Lü System. *Abstr. Appl. Anal.* **2015**, *2015*, 398027. [CrossRef]
25. Abbasbandy, S. Iterated He's Homotopy Perturbation Method for Quadratic Riccati Differential Equation. *Appl. Math. Comput.* **2006**, *175*, 581–589. [CrossRef]
26. Gökdogan, A.; Merdan, M. A Multistage Homotopy Perturbation Method for Solving Coullet System. *World Appl. Sci. J.* **2012**, *19*, 1813–1817.
27. Arciga-Alejandre, M.; Sánchez-Ortiz, J.; Ariza-Hernandez, F.; Catalan-Angeles, G. A Multi-Stage Homotopy Perturbation Method for the Fractional Lotka-Volterra Model. *Symmetry* **2019**, *11*, 1330. [CrossRef]
28. Roy, T.; Maiti, D. An Optimal and Modified Homotopy Perturbation Method for Strongly Nonlinear Differential Equations. *Nonlinear Dyn.* **2023**, *111*, 15215–15231. [CrossRef]
29. Manea, A.-S.; Stroita, D.-C.; Bordeasu, I.; Ghera, C.; Luca, A.-N. Air-Dynamic Measurements on "S" Shape Hydrofoils. *Mech. Mach. Sci.* **2025**, *174*, 47–56. [CrossRef]

30. Stroita, D.-C.; Bordeasu, D.; Dragan, F. System Identification of a Servo-Valve Controlled Hydraulic Cylinder Operating Under Variable Load. *Mathematics* **2025**, *13*, 341. [CrossRef]
31. Marinca, V.; Herisanu, N. *The Optimal Homotopy Asymptotic Method—Engineering Applications*; Springer: Berlin/Heidelberg, Germany, 2015.
32. Marinca, V.; Herisanu, N. Nonlinear dynamic analysis of an electrical machine rotor-bearing system by the optimal homotopy perturbation method. *Comp. Math. Appl.* **2011**, *61*, 2019–2024. [CrossRef]
33. Marinca, V.; Ene, R.D.; Marinca, B. Optimal Homotopy Perturbation Method for nonlinear problems with applications. *Appl. Comp. Math.* **2022**, *21*, 123–136. [CrossRef]
34. Hansen, L.P. Large Sample Properties of Generalized Method of Moment Models. *Econometrica* **1982**, *50*, 1269–1286. [CrossRef]
35. Den Haan, W.J.; Marcet, M. Accuracy in Simulations. *Rev. Econ. Stud.* **1994**, *61*, 3–17. [CrossRef]
36. King, M.R.; Mody, N.A. *Numerical and Statistical Methods for Bioengineering*; Cambridge University Press: Cambridge, UK, 2010; p. 594, ISBN 978-0-521-87158-7.
37. Ding, J.; Zhou, A. *Statistical Properties of Deterministic Systems*; Springer: Berlin/Heidelberg, Germany; New York, NY, USA, 2009; ISBN 978-3-540-85366-4.
38. Spagnolini, U. *Statistical Signal Processing in Engineering*; Wiley: Hoboken, NJ, USA, 2017; ISBN 9781119293996.
39. Ene, R.D.; Negrea, R.; Badarau, R.; Pop, N. Closed-form heteroclinic orbits for a three-parameter dynamical system using a modified Optimal Parametric Iteration Method. *Mathematics* **2026**, *14*, 1126. [CrossRef]
40. Ene, R.D.; Negrea, R.; Badarau, R.; Pop, N. Closed-form almost periodical solutions for a dynamical system using the Optimal Auxiliary Functions Method. *Mathematics* **2026**, *14*, 1260. [CrossRef]
41. Cox, D.R.; Snell, E.J. A general definition of residuals. *J. R. Stat. Soc. Ser. B* **1968**, *30*, 248–265. [CrossRef]
42. Yonar, A.; Yonar, H.; Demirsöz, M.; Tekindal, M.A. A comparative analysis for homogenity of varaince tests. *J. Sci. Arts* **2024**, *24*, 305–328. [CrossRef]
43. Wang, Y.; Rodriguez de Gil, P.; Chen, Y.H.; Kromrey, J.D.; Kim, E.S.; Pham, T.; Nguyen, D.; Romano, J.L. Comparing the Performance of Approaches for Testing the Homogeneity of Variance Assumption in One-Factor ANOVA Models. *Educ. Psychol. Meas.* **2017**, *77*, 305–329. [CrossRef] [PubMed]
44. Zhou, Y.; Zhu, Y.; Wong, W.K. Statistical tests for homogeneity of variance for clinical trials and recommendations. *Contemp. Clin. Trials Commun.* **2023**, *33*, 101119. [CrossRef] [PubMed]
45. Jarque, C.M.; Bera, A.K. Efficient tests for normality, homoscedasticity and serial independence of regression residuals. *Econ. Lett.* **1980**, *6*, 255–259. [CrossRef]

Disclaimer/Publisher's Note: The statements, opinions and data contained in all publications are solely those of the individual author(s) and contributor(s) and not of MDPI and/or the editor(s). MDPI and/or the editor(s) disclaim responsibility for any injury to people or property resulting from any ideas, methods, instructions or products referred to in the content.